

Sea-Surface Temperature from MODIS

Peter J Minnett, Robert H Evans and Gui Podestá

Meteorology and Physical Oceanography
Rosenstiel School of Marine and Atmospheric Science
University of Miami

UNIVERSITY OF MIAMI



Overview

- Sea-surface temperature (SST) as an Essential Climate Variable (ECV), and Climate Data Record (CDR)
- MODIS SSTs
 - Improvements in the atmospheric correction algorithms
- Radiometric measurements of SSTs from ships
 - Traceability to SI standards
- Physical processes at the sea surface
 - Diurnal heating and cooling
 - Thermal skin effect



Sea-surface temperature

- Temperature is a fundamental SI variable.
- SST is an important variable, helps determine the coupling between ocean and atmosphere.
- Has many applications in NWP, operational oceanography, climate studies.
- Can be measured to good accuracy from space.
- Can be validated to determine residual uncertainties.



Essential Climate Variables

GCOS
Global Climate Observing System

News Contact Publications Calendar Site map

WHO IOC LINP ICSU

Google Custom Search Search

GCOS Essential Climate Variables

The Essential Climate Variables (ECVs) are required to support the work of the UNFCCC and the IPCC. All ECVs are technically and economically feasible for systematic observation. It is these variables for which international exchange is required for both current and historical observations. Additional variables required for research purposes are not included in this table. It is emphasized that the ordering within the table is simply for convenience and is not an indicator of relative priority. Currently, there are 44 ECVs plus soil moisture recognized as an emerging ECV.

Domain	Essential Climate Variables
Atmospheric (over land, sea and ice)	Surface: Air temperature, Precipitation, Air pressure, Surface radiation budget, Wind speed and direction, Water vapour.
	Upper-air: Earth radiation budget (including solar irradiance), Upper-air temperature (including MSU radiances), Wind speed and direction, Water vapour, Cloud properties.
	Composition: Carbon dioxide, Methane, Ozone, Other long-lived greenhouse gases ^[1] , Aerosol properties.
Oceanic	Surface: Sea-surface temperature, Sea-surface salinity, Sea level, Sea state, Sea ice, Current, Ocean colour (for biological activity), Carbon dioxide partial pressure.
	Sub-surface: Temperature, Salinity, Current, Nutrients, Carbon, Ocean tracers, Phytoplankton.
Terrestrial ^[2]	River discharge, Water use, Ground water, Lake levels, Snow cover, Glaciers and ice caps, Permafrost and seasonally-frozen ground, Albedo, Land cover (including vegetation type), Fraction of absorbed photosynthetically active radiation (fAPAR), Leaf area index (LAI), Biomass, Fire disturbance, Soil moisture ^[3] .

Essential Climate Variables

The Essential Climate Variables (ECVs;) are required to support the work of the UNFCCC and the IPCC. All ECVs are technically and economically feasible for systematic observation. It is these variables for which international exchange is required for both current and historical observations. Additional variables required for research purposes are not included in this

- News
- About GCOS
- ▼ Climate Observation Needs
 - UNFCCC and GCOS
 - UNFCCC Guidelines
 - GCOS Reports to UNFCCC
 - ▶ Essential Climate Variables
 - Climate Monitoring Principles

GCOS Essential Climate Variables

The Essential Climate Variables (ECVs;) are required to support the work of the UNFCCC and the IPCC. All ECVs are technically and economically feasible for systematic observation. It is these variables for which international exchange is required for both current and historical observations. Additional variables required for research purposes are not included in this table. It is emphasized that the ordering within the table is simply for convenience and is not an indicator of relative priority. Currently, there are 44 ECVs plus soil moisture recognized as an emerging ECV.

Sea-surface temperature

- Outreach
- Contact

Domain	Essential Climate Variables
Atmospheric (and ice)	Surface: Air temperature, Precipitation, Air pressure, Surface radiation budget, Wind speed and direction, Water vapour.
	Upper-air: Earth radiation budget (including solar irradiance), Upper-air temperature (including MSU radiances), Wind speed and direction, Water vapour, Cloud properties.
	Composition: Carbon dioxide, Methane, Ozone, Other long-lived greenhouse gases[1], Aerosol properties.
Oceanic	Surface: Sea-surface temperature, Sea-surface salinity, Sea level, Sea state, Sea ice, Current, Ocean colour (for biological activity), Carbon dioxide partial pressure.
	Sub-surface: Temperature, Salinity, Current, Nutrients, Carbon, Ocean tracers, Phytoplankton.
Terrestrial[2]	River discharge, Water use, Ground water, Lake levels, Snow cover, Glaciers and ice caps, Permafrost and seasonally-frozen ground, Albedo, Land cover (including vegetation type), Fraction of absorbed photosynthetically active radiation (fAPAR), Leaf area index (LAI), Biomass, Fire disturbance, Soil moisture[3].



Satellite-derived CDRs

- National Academy of Sciences Report (NRC, 2000): *“a data set designed to enable study and assessment of long-term climate change, with ‘long-term’ meaning year-to-year and decade-to-decade change. Climate research often involves the detection of small changes against a background of intense, short-term variations.”*
- *“Calibration and validation should be considered as a process that encompasses the entire system, from the sensor performance to the derivation of the data products. The process can be considered to consist of five steps:*
 - *instrument characterization,*
 - *sensor calibration,*
 - *calibration verification,*
 - *data quality assessment, and*
 - *data product validation.”*

Desired SST CDR uncertainties

- The useful application of all satellite-derived variables depends on a confident determination of uncertainties.
- CDRs of SSTs require most stringent knowledge of the uncertainties:
 - Target accuracies: **0.1K** over large areas, stability
0.04K/decade - Ohring et al. (2005) Satellite Instrument Calibration for Measuring Global Climate Change: Report of a Workshop. *Bulletin of the American Meteorological Society* **86**:1303-1313

What is SST?

- The infrared emission from the ocean originates from the uppermost <1mm of the ocean – the skin layer.
- The atmosphere is in contact with the top of the skin layer.
- Ocean-to-atmosphere heat flow through the skin layer is by molecular conduction: this causes, and results from, a temperature gradient through the skin layer.
- Conventional measurements of SST are from submerged thermometers – a “bulk” temperature.
- T_{depth} below the influence of diurnal heating is the “foundation” temperature.

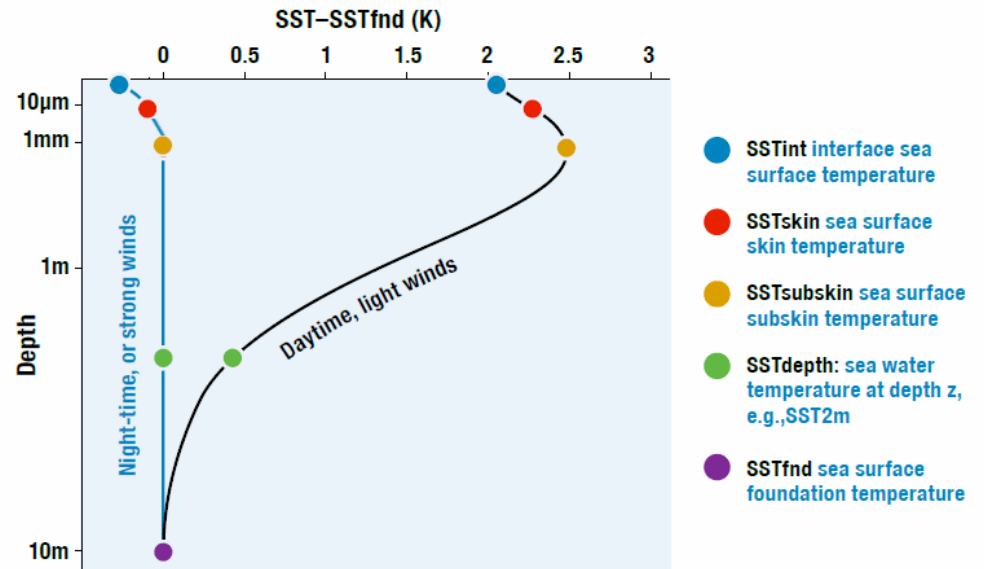
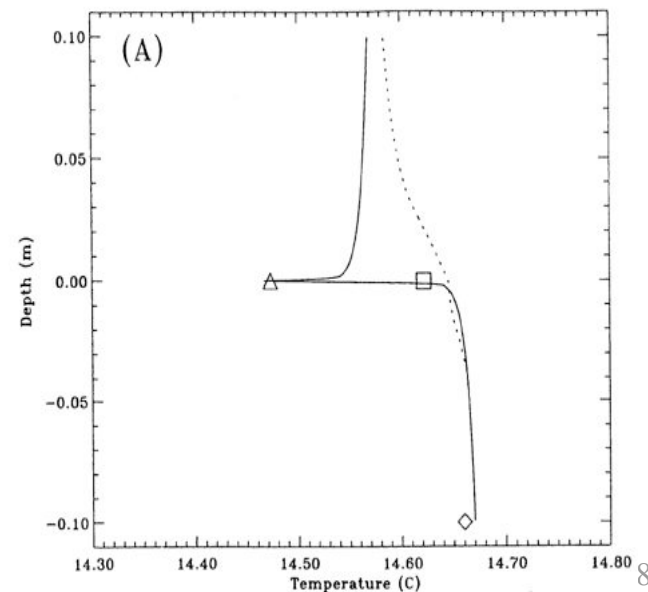


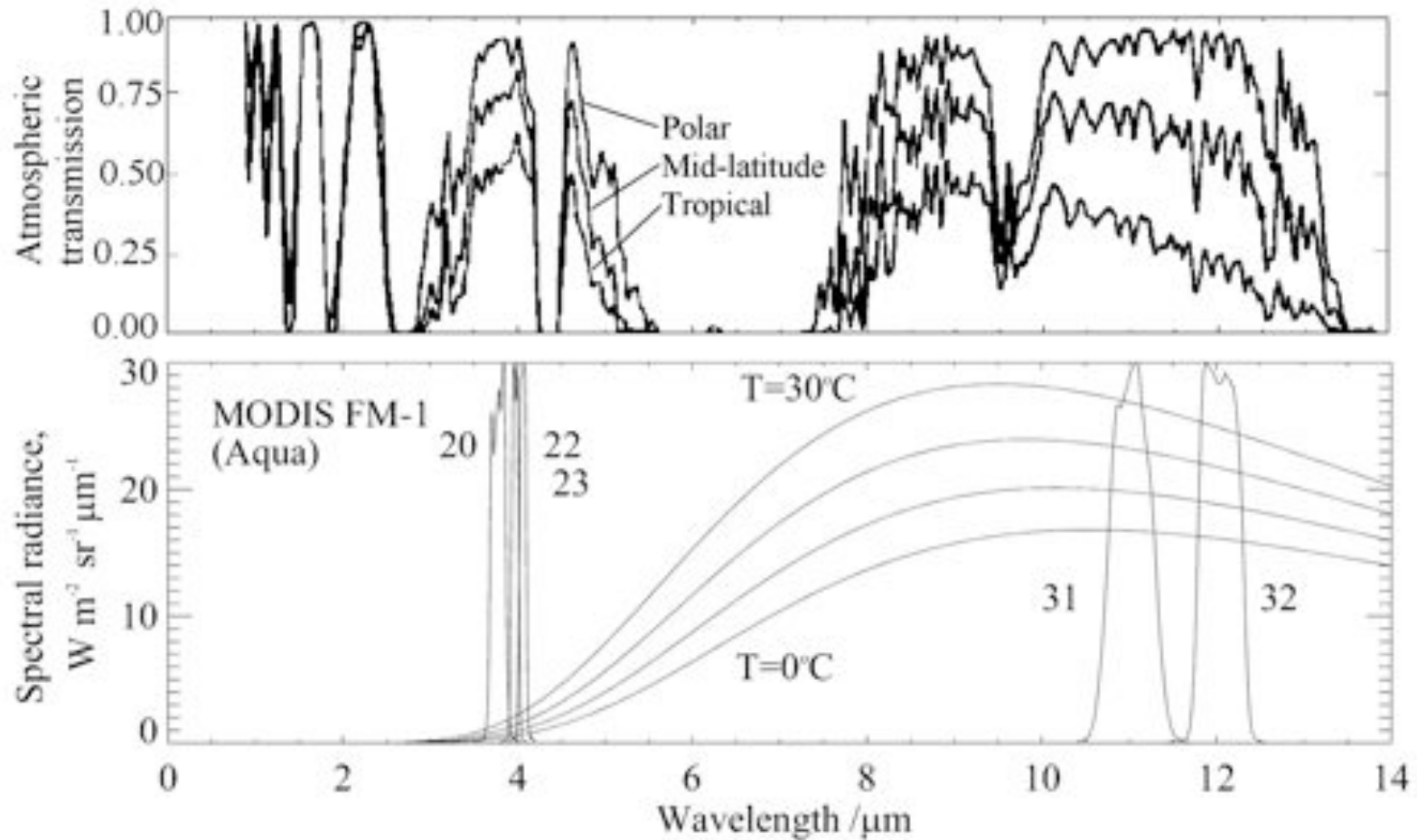
Figure 1: The hypothetical vertical profiles of temperature for the upper 10m of the ocean surface in high wind speed conditions or during the night (red) and for low wind speed during the day (black).



From Eifler, W. and C. J. Donlon, 2001: Modeling the thermal surface signature of breaking waves. *J. Geophys. Res.*, 106, 27,163-27,185.

Infrared measurement of SST

MODIS FM-1 Bands 20, 22, 23, 31 & 32



The SST atmospheric correction algorithms

The form of the daytime and night-time algorithm for measurements in the long wave atmospheric window is:

$$SST = c_1 + c_2 * T_{11} + c_3 * (T_{11} - T_{12}) * T_{sfc} + c_4 * (\sec(\theta) - 1) * (T_{11} - T_{12})$$

where T_n are brightness temperatures measured in the channels at n μm wavelength, T_{sfc} is a 'climatological' estimate of the SST in the area, and θ is the satellite zenith angle. This is based on the Non-Linear SST algorithm.

[Walton, C. C., W. G. Pichel, J. F. Sapper and D. A. May (1998). "The development and operational application of nonlinear algorithms for the measurement of sea surface temperatures with the NOAA polar-orbiting environmental satellites." Journal of Geophysical Research **103** 27,999-28,012.]

The MODIS night-time algorithm, using two bands in the 4 μm atmospheric window is:

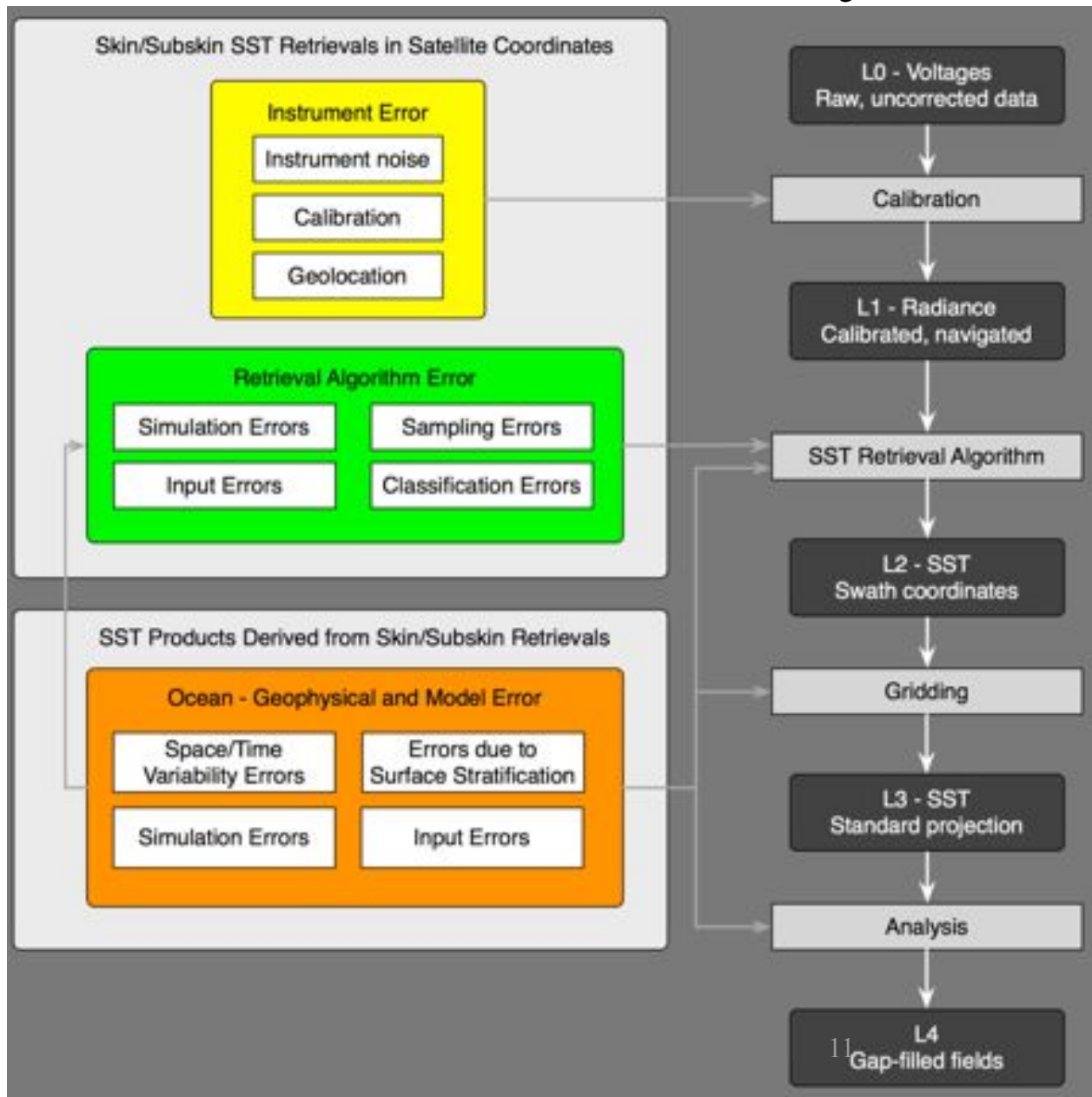
$$SST4 = c_1 + c_2 * T_{3.9} + c_3 * (T_{3.9} - T_{4.0}) + c_4 * (\sec(\theta) - 1)$$

Note, the coefficients in each expression are different. They can be derived in three ways:

- empirically by regression against SST values derived from another validated satellite instrument
- empirically by regression against SST values derived surface measurements from ships and buoys
- theoretically by numerical simulations of the infrared radiative transfer through the atmosphere.



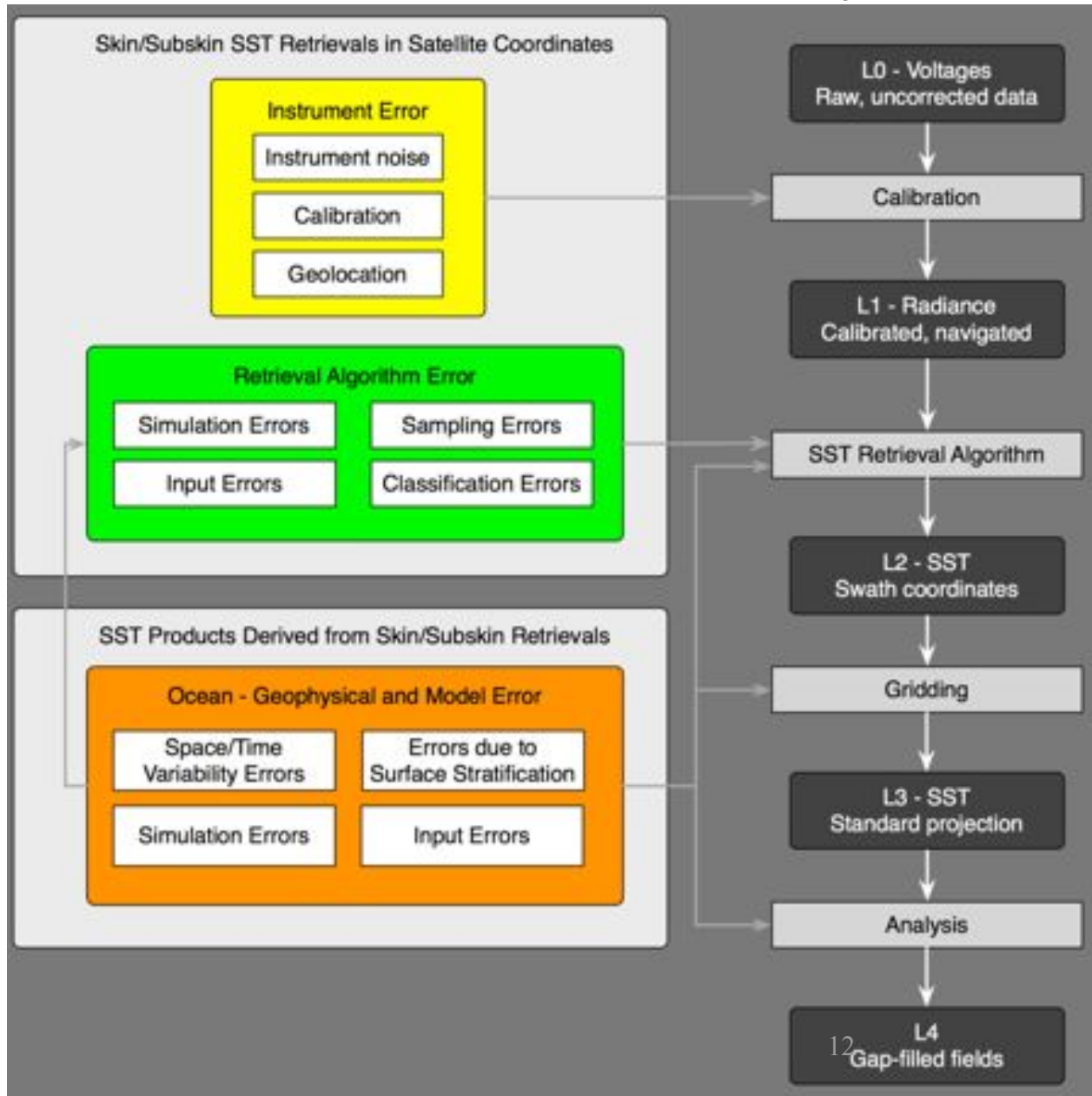
Uncertainty estimates



Each processing step is prone to additional error sources.

From Cornillon et al, 2010, Sea-Surface Temperature Error Budget White Paper. (<http://www.ssterrorbudget.org/ISSTST/>)

Uncertainty estimates

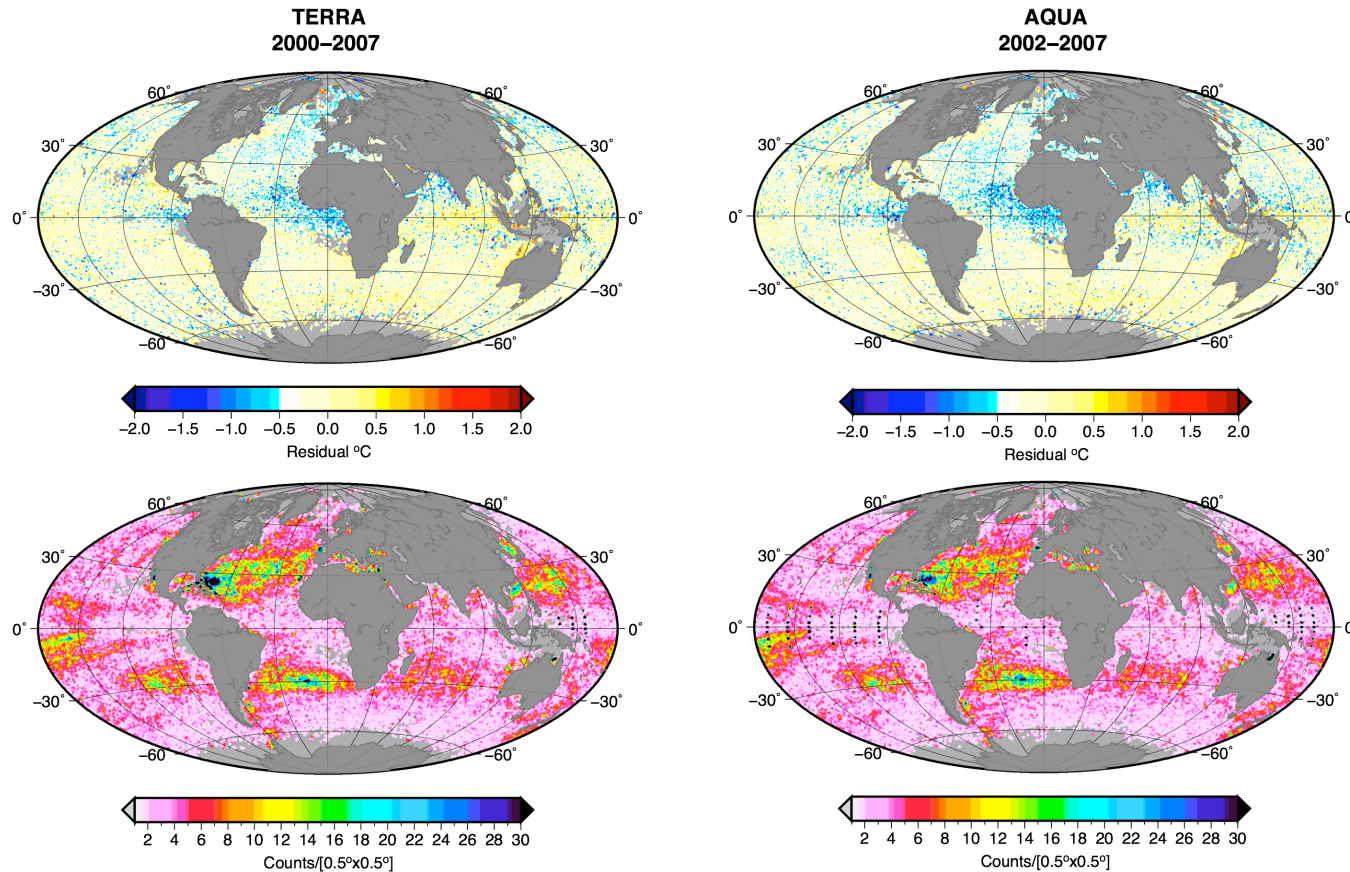


Each processing step is prone to additional error sources.



From Cornillon et al, 2010, Sea-Surface Temperature Error Budget White Paper. (<http://www.ssterrorbudget.org/ISSTST/>)

Spatial distribution of errors



Areas of high bias errors can be related to geophysical phenomena: aerosols, upwelling, diurnal heating, anomalous
dity distributions

Where next?

- Refine NLSST with regionally as well as seasonally optimized coefficient sets – “Latband algorithm”
- Use advanced computational techniques:
 - Genetic Algorithm (GA)-based equation discovery to derive alternative forms of the correction algorithm
 - Regression tree to identify geographic regions with related characteristics
 - Support Vector Machines (SVM) to minimize error using state-of-the-art non-linear regression



“Latband” improvements

Time series of mean SST residuals for MODIS-Aqua.

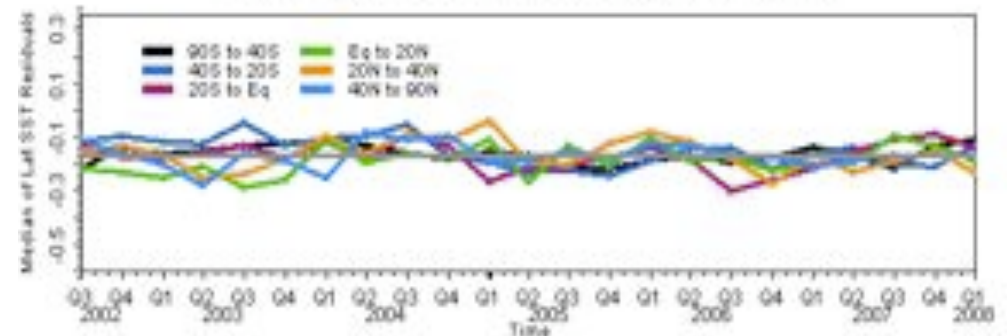
Algorithm coefficients estimated for six fixed latitudinal bands and for each month of the year.

V6 – with “LATBAND” approach.

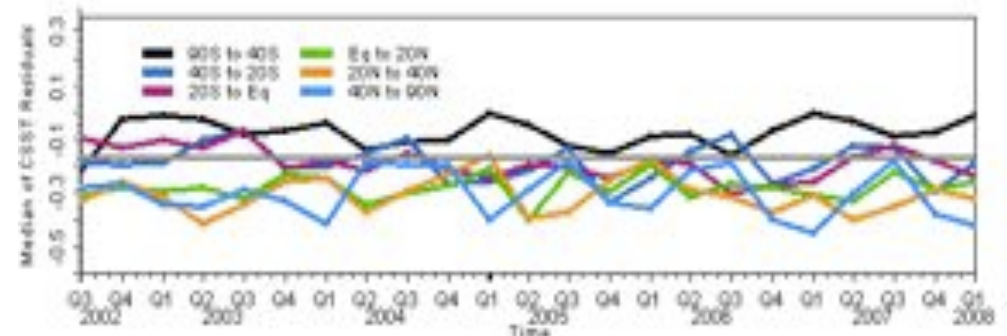
V5 – without.

Version 6

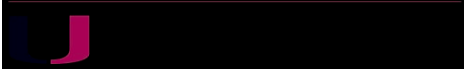
AQUA - Median of Lat SST Residuals by Latitude Band



AQUA - Median of CSST Residuals by Latitude Band



Version 5



Equation Discovery using Genetic Algorithms

- Darwinian principles are applied to algorithms that “mutate” between successive generations
- The algorithms are applied to large data bases of related physical variables to find robust relationships between them. Only the “fittest” algorithms survive to influence the next generation of algorithms.
- Here we apply the technique to the MODIS matchup-data bases.
- The survival criterion is the size of the RMSE of the SST retrievals when compared to buoy data.

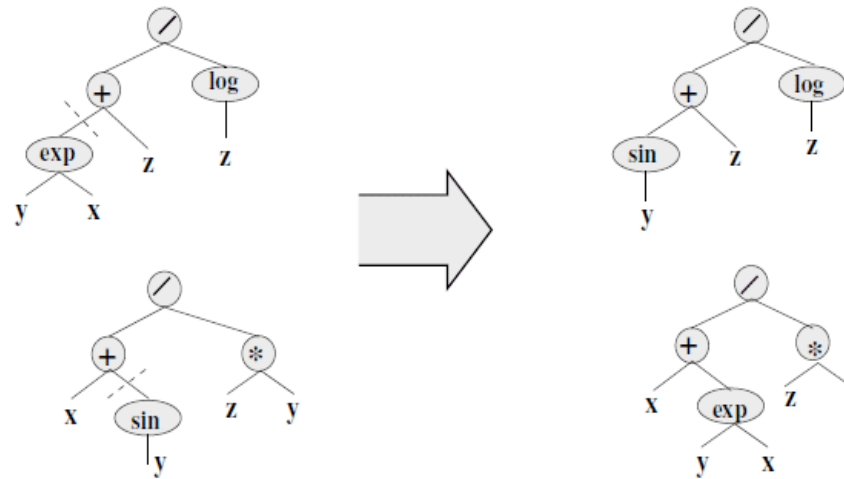


Genetic Mutation of Equations

- The **initial population** of formulae is created by a generator of random algebraic expressions from a predefined set of variables and operators. For example, the following operators can be used: $\{+, -, /, \times, \sqrt{\quad}, \exp, \cos, \sin, \log\}$. To the random formulae thus obtained, we can include “seeds” based on published formulae, such as those already in use.
- In the **recombination** step, the system randomly selects two parent formulae, chooses a random subtree in each of them, and swaps these subtrees.
- The **mutation of variables** introduces the opportunity to introduce different variables into the formula. In the tree that defines a formula, the variable in a randomly selected leaf is replaced with another variable.



Successive generations of algorithms



The formulae are represented by tree structures; the “recombination” operator exchanges random subtrees in the parents. Here the parent formulae $(y^x+z)/\log(z)$ and $(x+\sin(y))/zy$ give rise to children formulae $(\sin(y)+z)/\log(z)$ and $(x+y^x)/zy$. The affected subtrees are indicated by dashed lines.

Subsets of the data set can be defined in any of the available parameter spaces.

(From Wickramaratna, K., M. Kubat, and P. Minnett, 2008:
Discovering numeric laws, a case study: CO₂ fugacity in the ocean.
Intelligent Data Analysis, 12, 379-391.)

GA-based equation discovery

initial state: randomly generated formulas plus manually created “seed” formulas

1. Randomly selected mating partners exchange genetic information by the recombination operator.
 2. 20% randomly selected individuals are subjected to mutation of variables; 20% randomly selected individuals are subjected to mutation of operators; and all individuals are subjected to mutation of coefficients.
 3. All individuals are subjected to mutation of inter-region borders.
 4. The fitness of each individual (children as well as parents) is calculated as the formula's error on the training data. The top 50% are retained, and the remaining formulas are discarded.
 5. Unless a termination criterion is satisfied, return to step 1.
-

And the winner is....



And the winner is....

The “fittest” algorithm takes the form:

$$SST = c_0 + c_1 T_{11} + c_2 (T_{11} - T_{12}) T_4 + \frac{c_3 (T_{11} - T_{12})}{\cos(1.13 \times \theta_s)} + c_4 \times \cos(1.0078 \times \theta_a - 0.7099)$$

where:

T_i is the brightness temperature at $\lambda = i \mu\text{m}$

θ_s is the satellite zenith angle

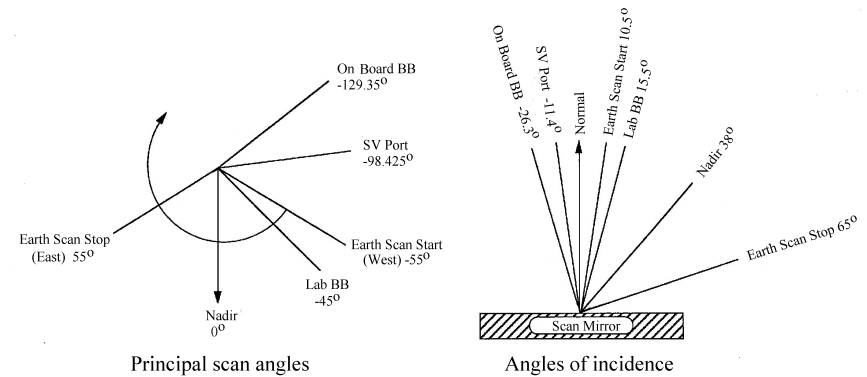
θ_a is the angle on the mirror (a feature of the MODIS paddle-wheel mirror design)

Which looks similar to the NLSST:

Non-Linear SST (NLSST)

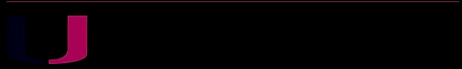
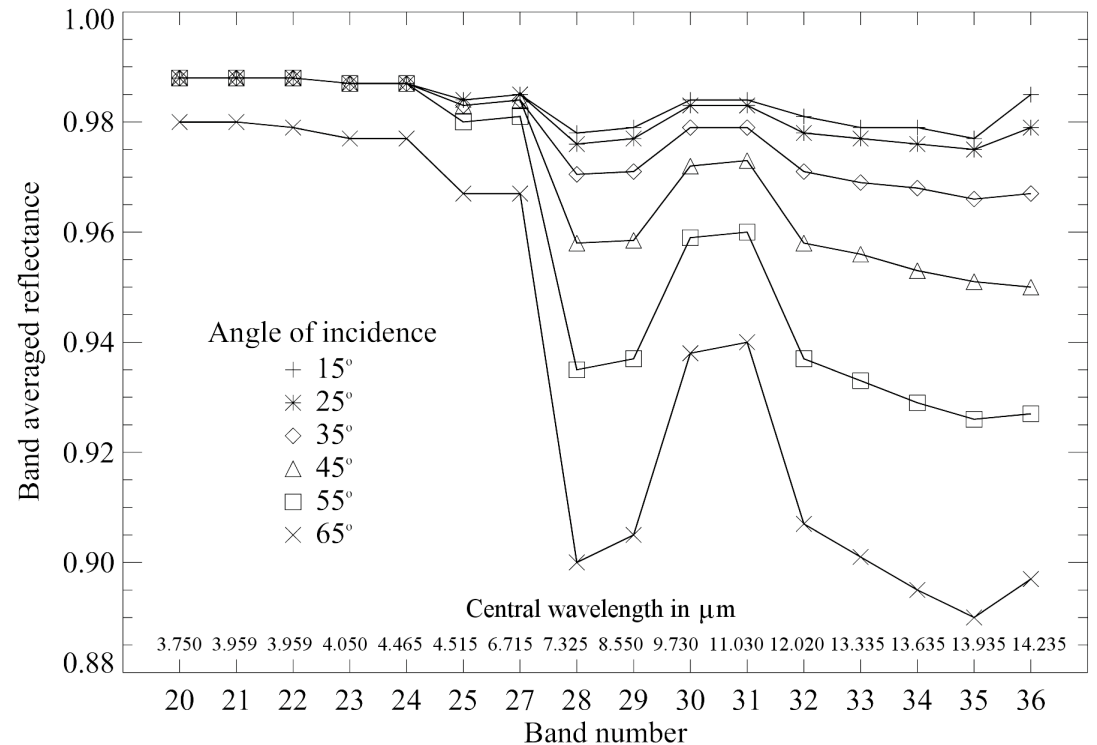
$$NLSST = b_0 + b_1 * T_{11} + b_2 * T_{37} * (T_{11} - T_{12}) + b_3 * (T_{11} - T_{12}) * (\sec(\theta) - 1.)$$

MODIS scan mirror effects



Mirror effects: two-sided paddle wheel has a multi-layer coating that renders the reflectivity in the infrared a function of wavelength, angle of incidence and mirror side.

Terra MODIS Scan Mirror Reflectance



Variants of the new algorithms

- * Terra SST4:

$$SST = c_0 + c_1 T_{4.0} + c_2 (T_{3.9} - T_{4.0}) T_{3.9} + \frac{c_3 (T_{3.9} - T_{4.0})}{\cos(1.13 \times \theta_s)} + c_4 \times \cos(1.0078 \times \theta_a - 0.7099)$$

- * Terra SSTnight, SSTday, SST:

$$SST = c_0 + c_1 T_{11} + c_2 (T_{11} - T_{12}) + \frac{c_3 (T_{11} - T_{12})}{\cos(1.13 \times \theta_s)} + c_4 \times \cos(1.0078 \times \theta_a - 0.7099)$$

- * Terra newSSTnight:

$$SST = c_0 + c_1 T_{3.9} + c_2 (T_{3.9} - T_{4.0}) + \frac{c_3 (T_{3.9} - T_{4.0})}{\cos(1.13 \times \theta_s)} + c_4 \times \cos(1.0078 \times \theta_a - 0.7099)$$

- * Aqua SST4:

$$SST = c_0 + c_1 T_{3.9} + c_2 (T_{3.9} - T_{4.0}) T_{3.9} + \frac{c_3 (T_{3.9} - T_{4.0})}{\cos(1.13 \times \theta_s)} + c_4 \times \cos(1.0078 \times \theta_a - 0.7099)$$

- * Aqua SSTnight, SSTday, SST:

$$SST = c_0 + c_1 T_{11} + c_2 (T_{11} - T_{12}) + \frac{c_3 (T_{11} - T_{12})}{\cos(1.13 \times \theta_s)} + c_4 \times \cos(1.0078 \times \theta_a - 0.7099)$$

- * Aqua newSSTnight:

$$SST = c_0 + c_1 T_{3.8} + c_2 (T_{11} - T_{12}) T_{3.9} + \frac{c_3 (T_{11} - T_{12})}{\cos(1.13 \times \theta_s)} + c_4 \times \cos(1.0078 \times \theta_a - 0.7099)$$

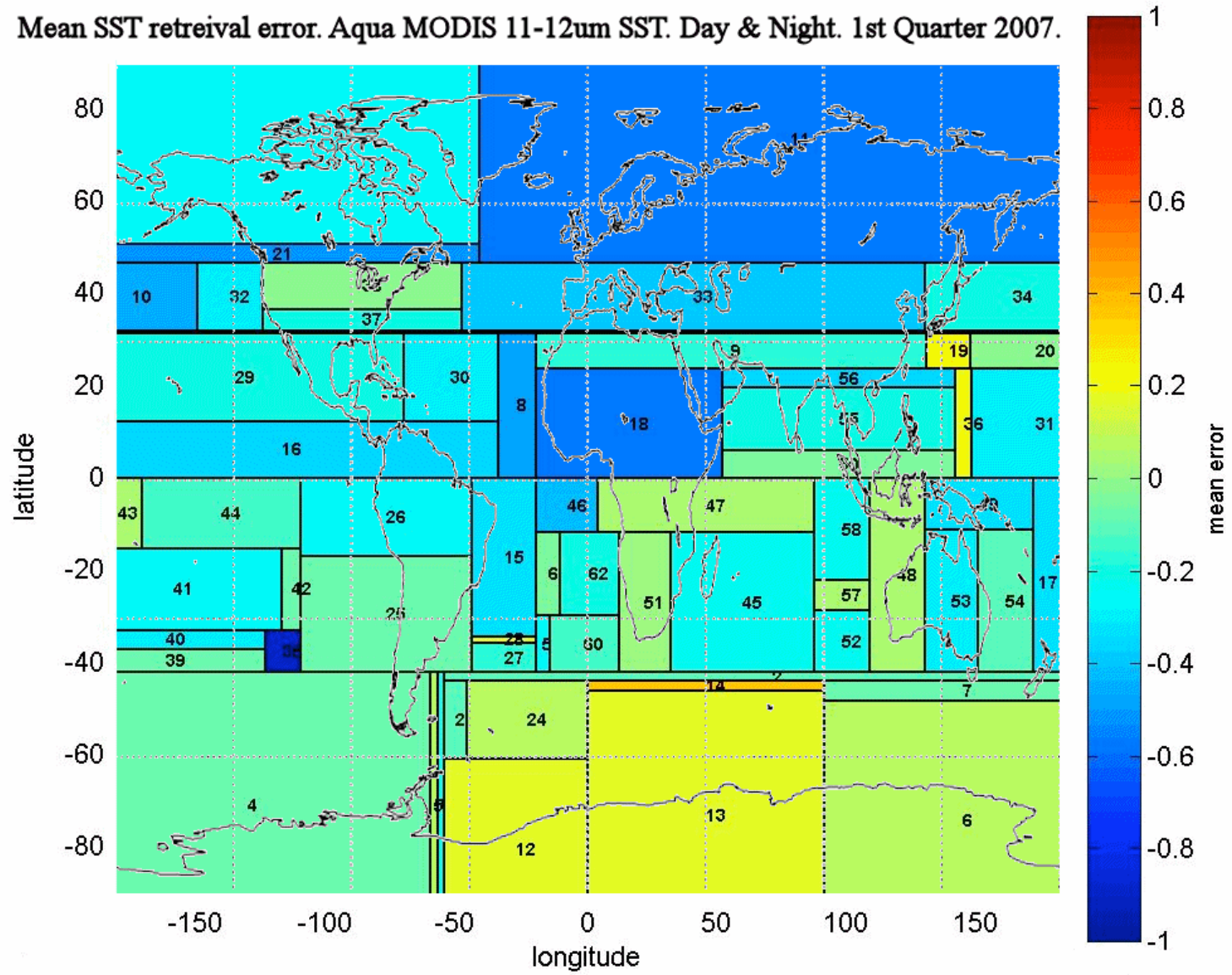
Coefficients are different for each equation

Note: No T_{sfc}

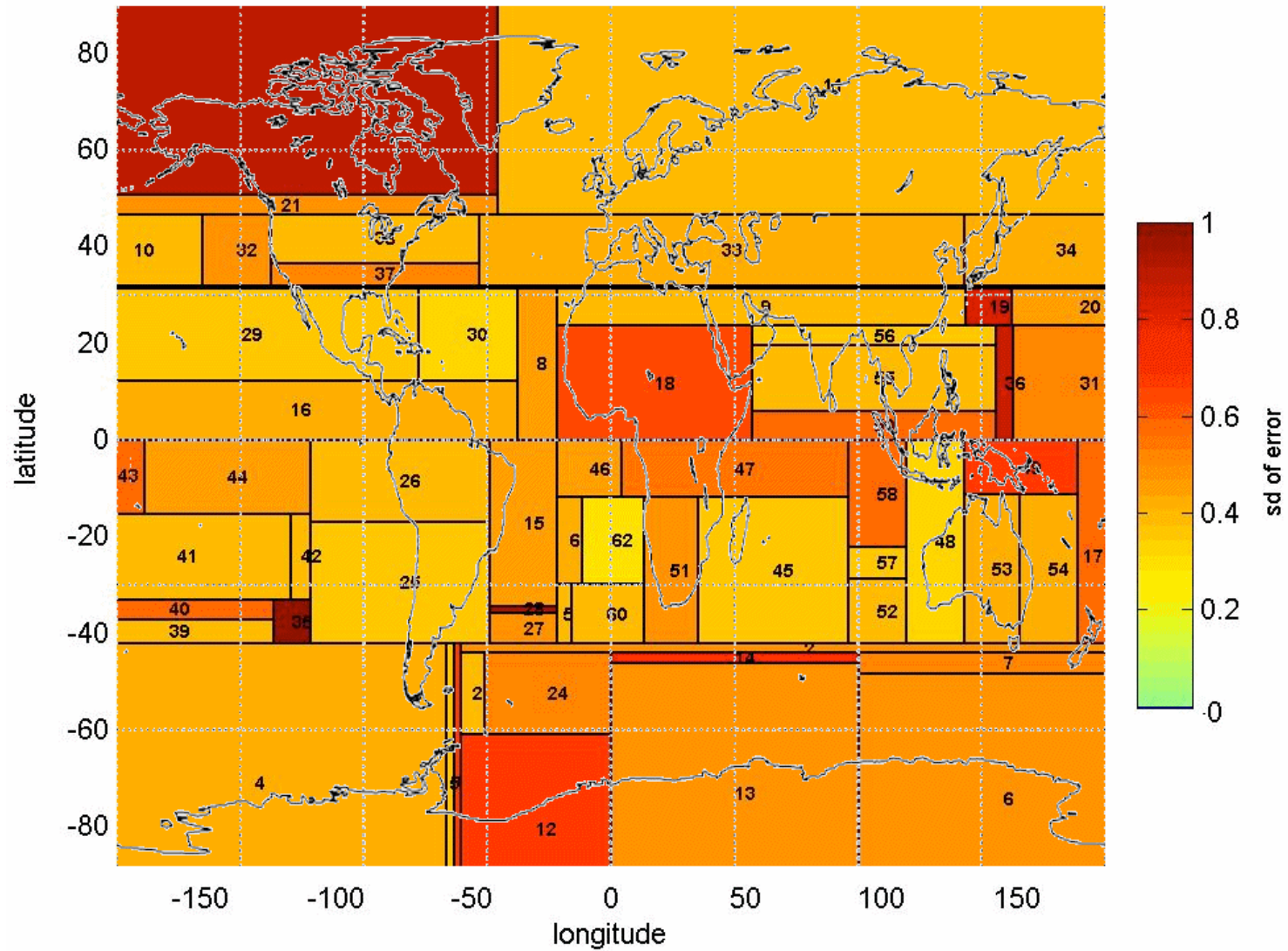
Regression tree

- Regions identified by the regression tree algorithm
- The tree is constructed using
 - input variables: latitude and longitude
 - output variable: *Error in retrieved SST*
- Algorithm recursively splits regions to minimize variance within them
- The obtained tree is pruned to the smallest tree within one standard error of the minimum-cost subtree, provided a declared minimum number of points is exceeded in each region
- Linear regression is applied separately to each resulting region (different coefficients result)

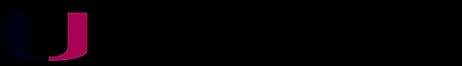
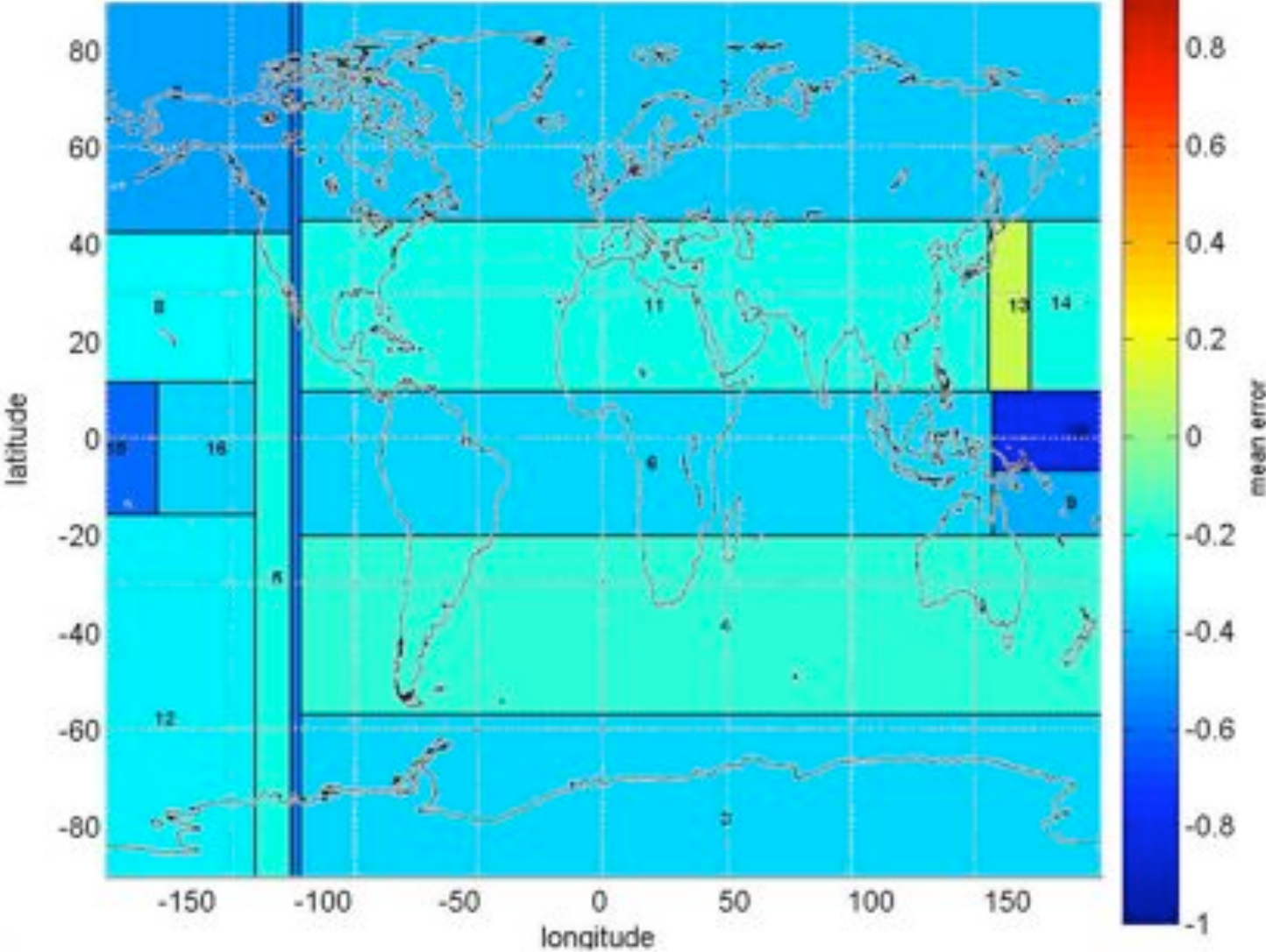
Mean SST retrieval error. Aqua MODIS 11-12um SST. Day & Night. 1st Quarter 2007.



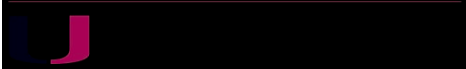
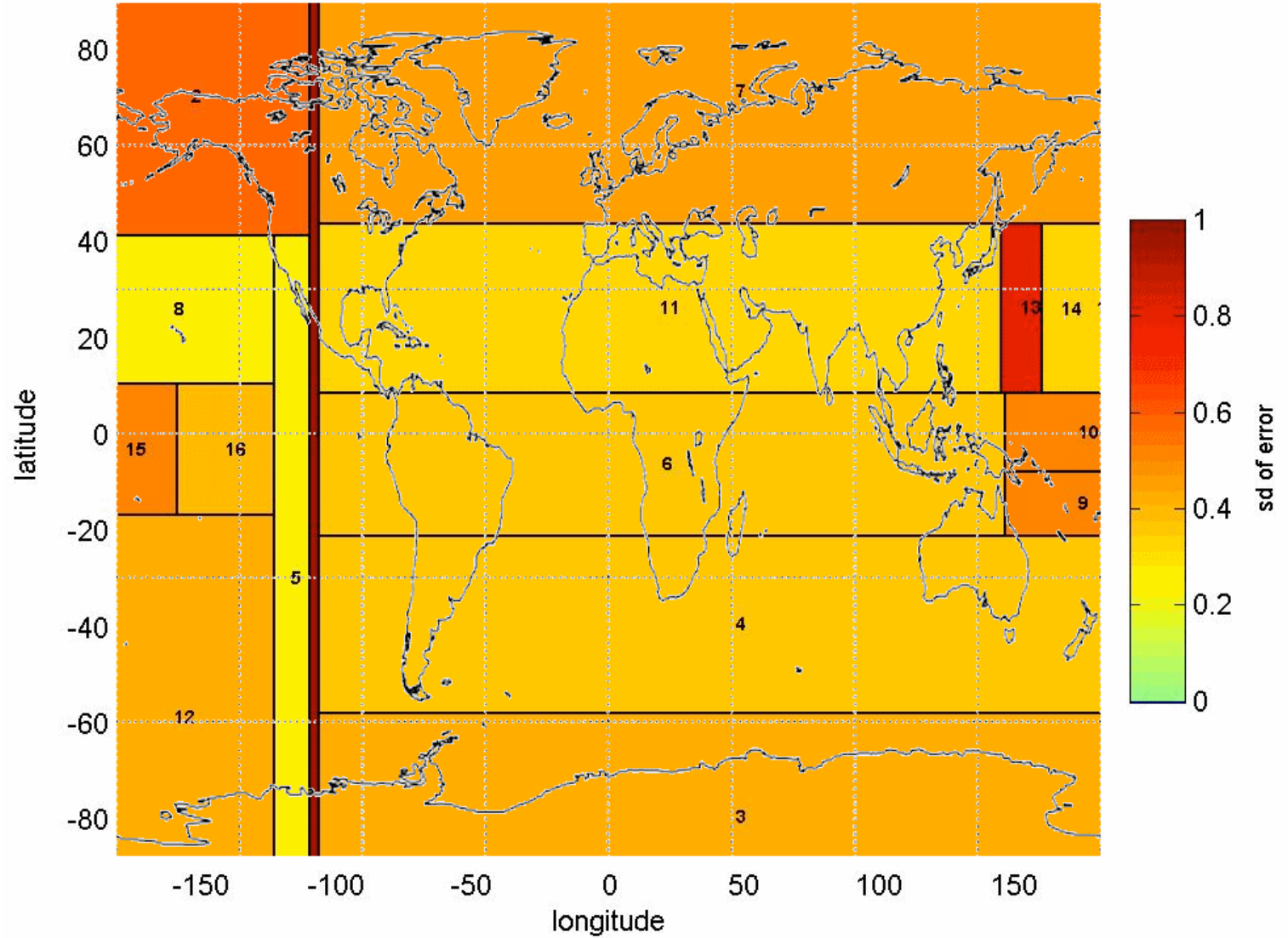
Std. Dev of SST retrieval error. Aqua MODIS 11-12um SST. Day & Night. 1st Quarter 2007.



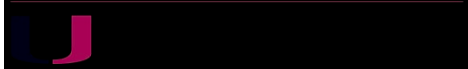
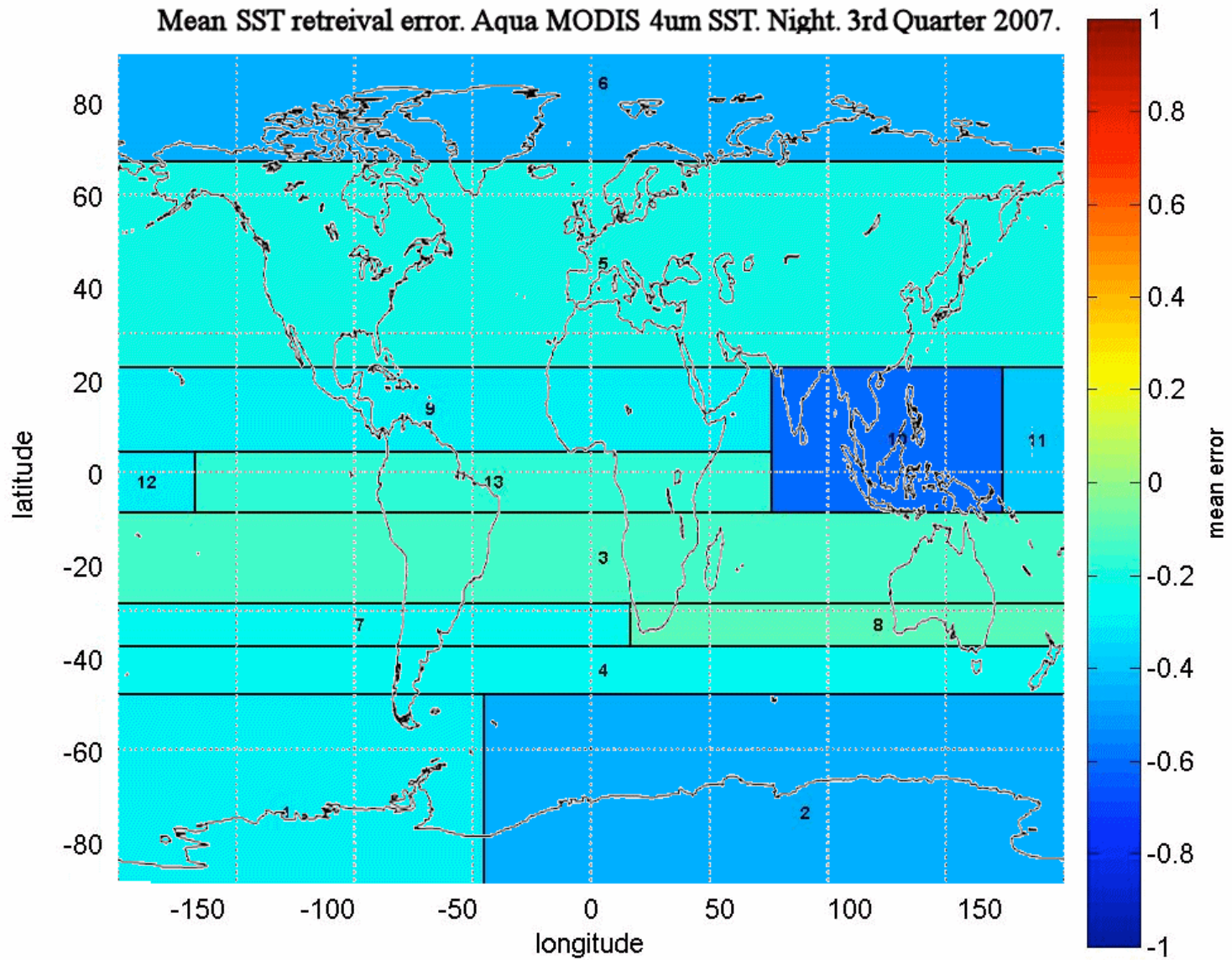
Mean SST retrieval error. Aqua MODIS 4um SST. Night - 1st Quarter. 2007



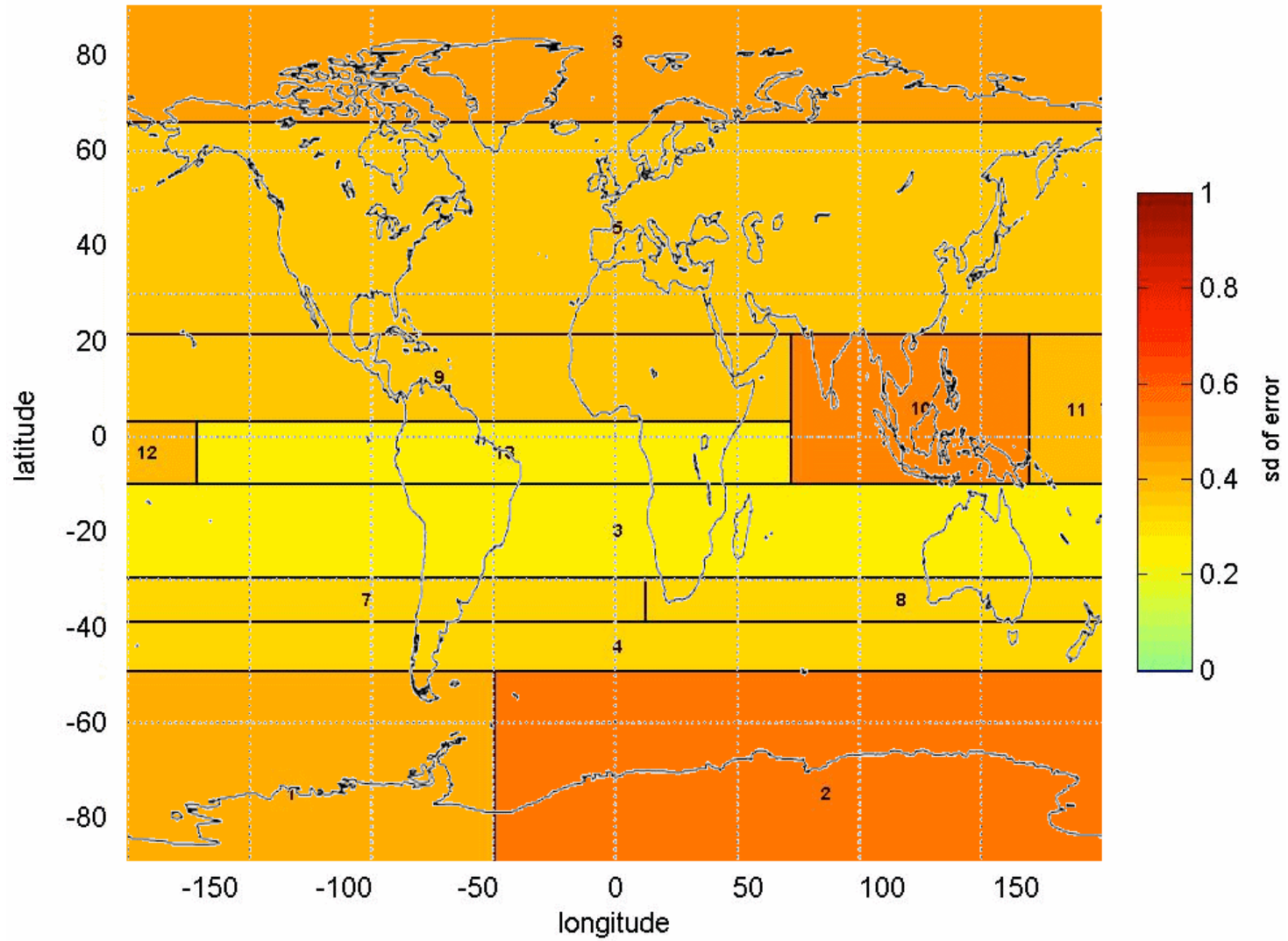
Std. Dev of SST retrieval error. Aqua MODIS 4um SST. Night. 1st Quarter 2007.



Mean SST retrieval error. Aqua MODIS 4um SST. Night. 3rd Quarter 2007.



Std. Dev of SST retrieval error. Aqua MODIS 4um SST. Night. 3rd Quarter 2007.



Regression tree performance

- Terra 2004 SSTday

NLSST (no regions) – RMSE: 0.581

New formula (no regions) – RMSE: 0.615

New formula (with regions) – RMSE: 0.568

- Terra 2004 SST4 (night)

SST4 (no regions) – RMSE: 0.528

New formula (no regions) – RMSE: 0.480

New formula (with regions) – RMSE: 0.456



Support Vector Machines (SVM)

- Best accuracy observed when data set is large (lower accuracy when splitting into regions)
 - Terra 2004 SSTday –
 - RMSE (no region): 0.513, RMSE (with regions): 0.557
- Problems:
 - Computational costs
 - Black-box approach

Preliminary Results

- The new algorithms with regions give smaller errors than NLSST or SST₄
- T_{sfc} term no longer required
- Night-time 4 μ m SSTs give smallest errors
- Aqua SSTs are more accurate than Terra SSTs
- Regression-tree induced in one year can be applied to other years without major increase in uncertainties
- SVM results do not out-perform GA+Regression Tree algorithms

Next steps

- Can some regions be merged without unacceptable increase in uncertainties?
- 180°W should not necessarily always be a boundary of all adjacent regions.
- Iterate back to GA for regions – different formulations may be more appropriate in different regions.
- Allow scan-angle term to vary with different channel sets.
- Introduce “regions” that are not simply geographical.



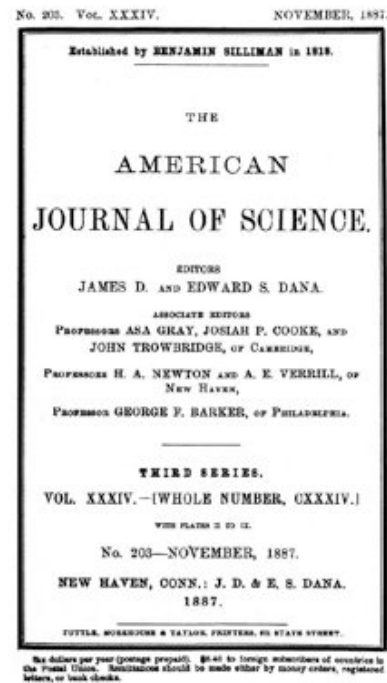
Validation and CDR generation

- Validation required over life-time of mission
- Should encompass all atmospheric and oceanic variability.
- Traceability to SI standards is needed.

→ ship-based radiometers

Marine-Atmospheric Emitted Radiance Interferometer

The M-AERI is a Michelson-Morley Fourier-transform infrared interferometric spectroradiometer. These were first developed in the 1880's to make accurate measurements of the speed of light. Here we use it to make very accurate measurements of the sea-surface temperature, air temperature and profiles of atmospheric temperature and humidity. We also measure surface emissivity and the temperature profile through the skin layer, which is related to the flow of heat from the ocean to the atmosphere.



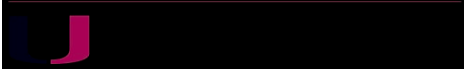
THE
AMERICAN JOURNAL OF SCIENCE.

[THIRD SERIES.]

ART. XXXVII.—On the Relative Motion of the Earth and the Luminiferous Ether; by ALBERT A. MICHELSON and EDWARD W. MORLEY.*

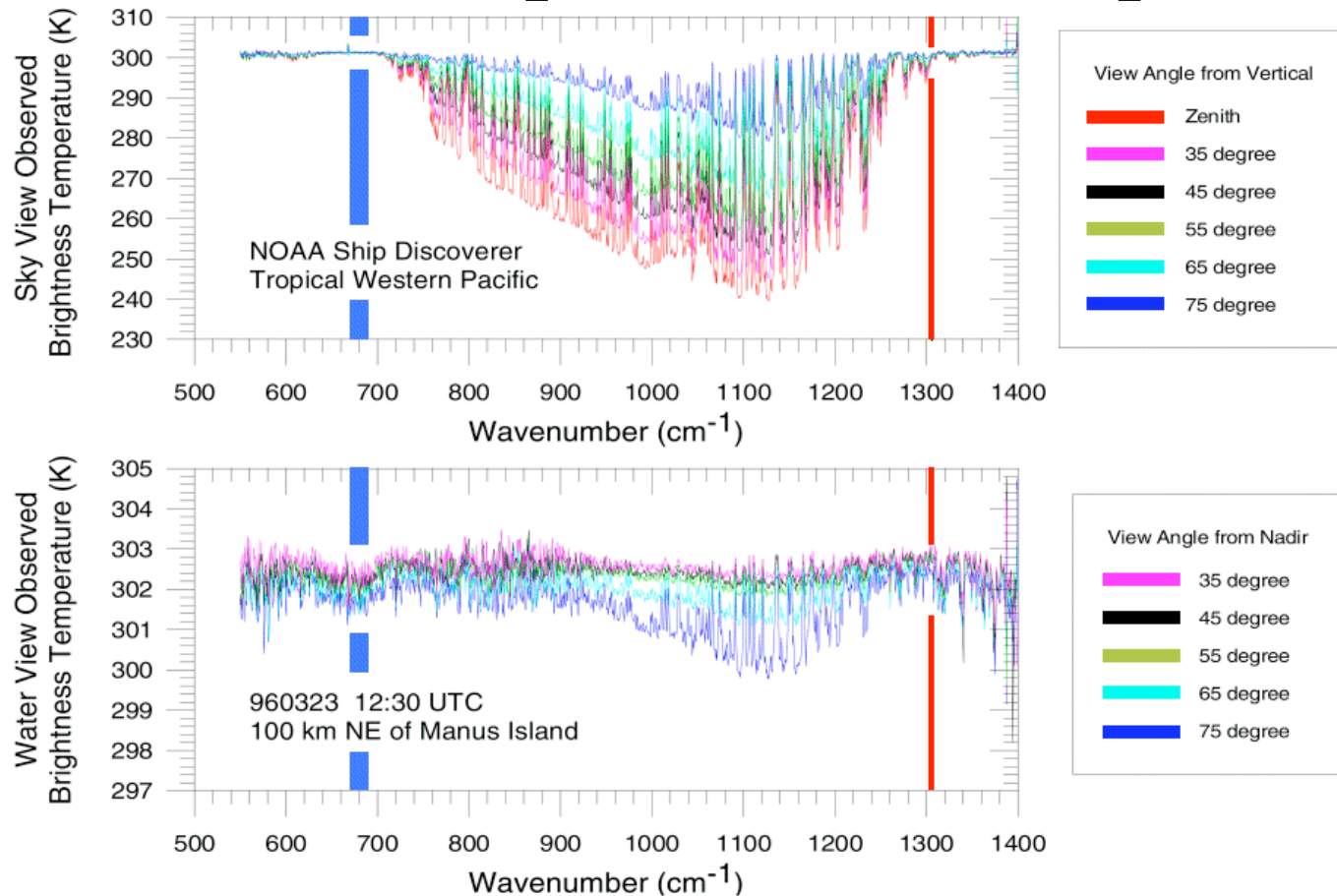
THE discovery of the aberration of light was soon followed by an explanation according to the emission theory. The effect was attributed to a simple composition of the velocity of light with the velocity of the earth in its orbit. The difficulties in this apparently sufficient explanation were overlooked until after an explanation on the undulatory theory of light was proposed. This new explanation was at first almost as simple as the former. But it failed to account for the fact proved by experiment that the aberration was unchanged when observations were made with a telescope filled with water. For if the tangent of the angle of aberration is the ratio of the velocity of the earth to the velocity of light, then, since the latter velocity in water is three-fourths its velocity in a vacuum, the aberration observed with a water telescope should be four-fifths of its true value.†

* This research was carried out with the aid of the Warde Fund.
† It may be added that most writers admit the sufficiency of the explanation according to the emission theory of light; while in fact the difficulty is even greater than according to the undulatory theory. For on the emission theory the velocity of light must be greater in the water telescope, and therefore the angle of aberration should be less; hence, in order to reduce it to its true value, we must make the absurd hypothesis that the motion of the water in the telescope carries the ray of light in the opposite direction!
Am. Jour. Sci.—Third Series, Vol. XXXIV, No. 203.—Nov., 1887.
11



Ocean and atmosphere infrared spectra

NB: X10 change in temperature scale



Examples of parts of spectra measured by the M-AERI, represented as temperature, and those intervals where the sky temperatures are smallest indicate where the atmosphere is most transparent. The spikes in the atmospheric spectra are caused by emission lines. The blue bar shows which spectral region is used to measure air temperature, and the red bar skin sea-ice temperature. Note the change in temperature scales of the two panels. These data were taken in the Tropical Western Pacific during the Combined Sensor Program Cruise in 1996.

Marine-Atmospheric Emitted Radiance Interferometer (M-AERI)



Specifications

Spectral interval	~3 to ~18 μ m
Spectral resolution	0.5 cm ⁻¹
Interferogram rate	1Hz
Aperture	2.5 cm
Detectors	InSb, HgCdTe
Detector temperature	78°K
Calibration	Two black-body cavities
SST retrieval uncertainty	<< 0.1K (absolute)

Laboratory tests of M-AERI accuracy

Target Temp.	LW (980-985 cm ⁻¹)	SW (2510-2515 cm ⁻¹)
20°C	+0.013 K	+0.010 K
30°C	-0.024 K	-0.030 K
60°C	-0.122 K	-0.086 K

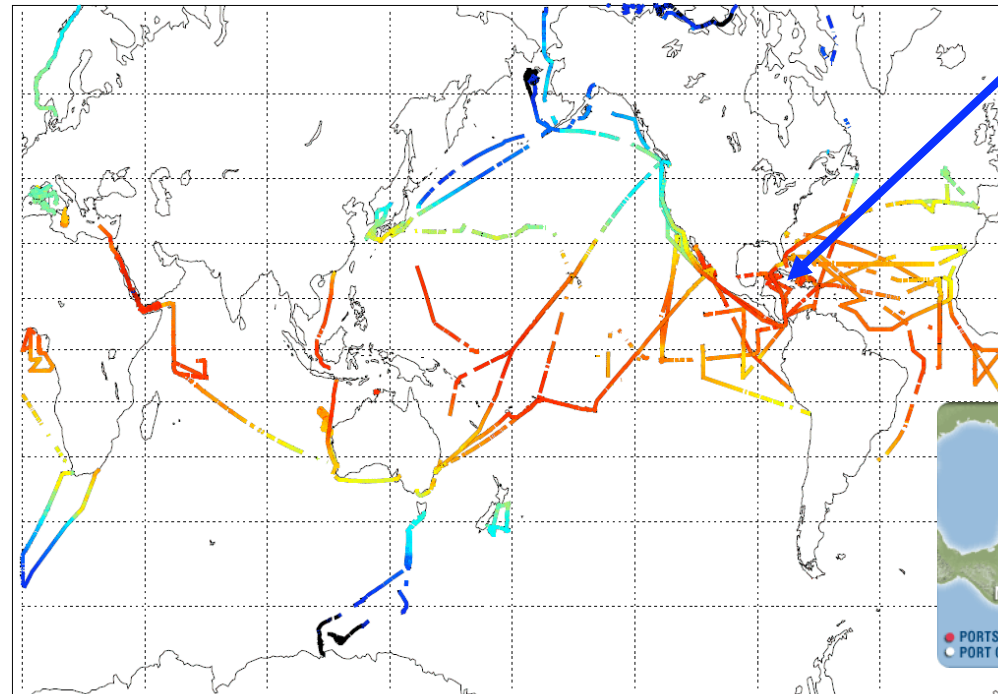
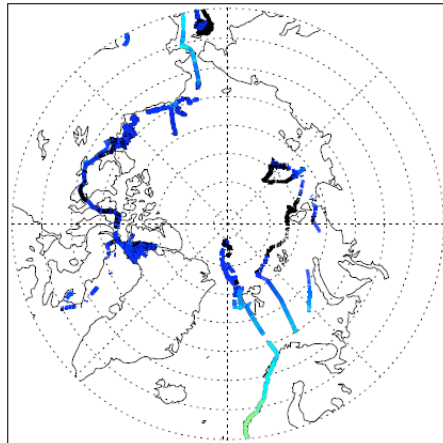
The mean discrepancies in the M-AERI O₂ measurements of the NIST water bath blackbody calibration target in two spectral intervals where the atmosphere absorption and emission are low. Discrepancies are M-AERI minus NIST temperatures.



M-AERI on USCGC *Polar Star*, March 2000



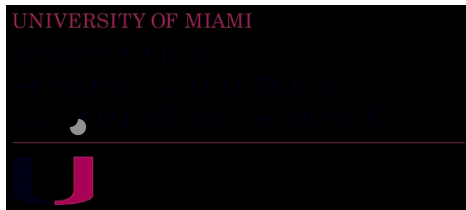
M-AERI cruises for MODIS, AATSR & AVHRR validation



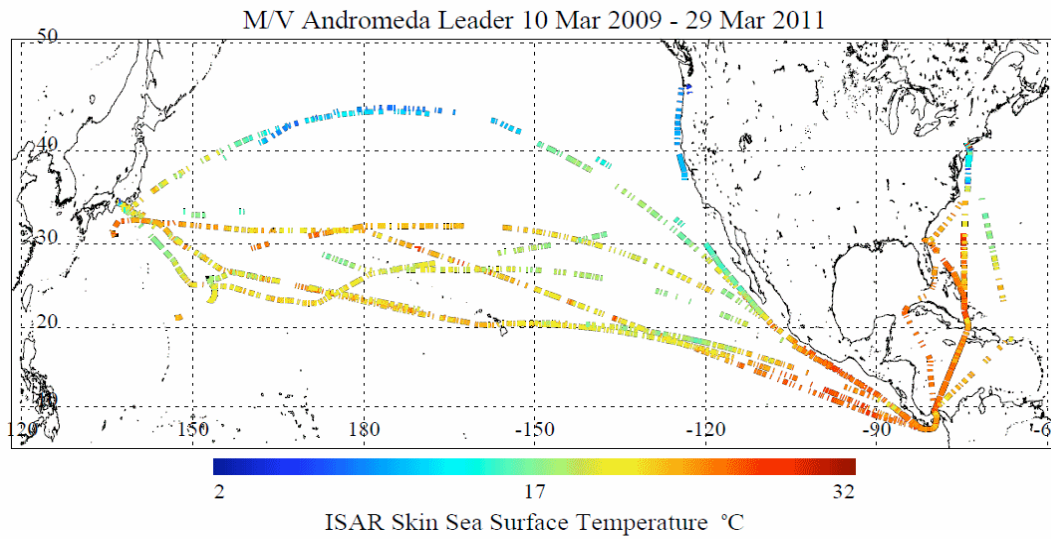
Explorer of the Seas



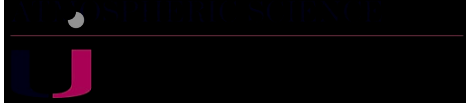
Explorer of the Seas: near continuous operation December 2000 – December 2007. Restarted February 2010.



ISAR cruises for MODIS, AATSR & AVHRR validation



UNIVERSITY OF MIAMI

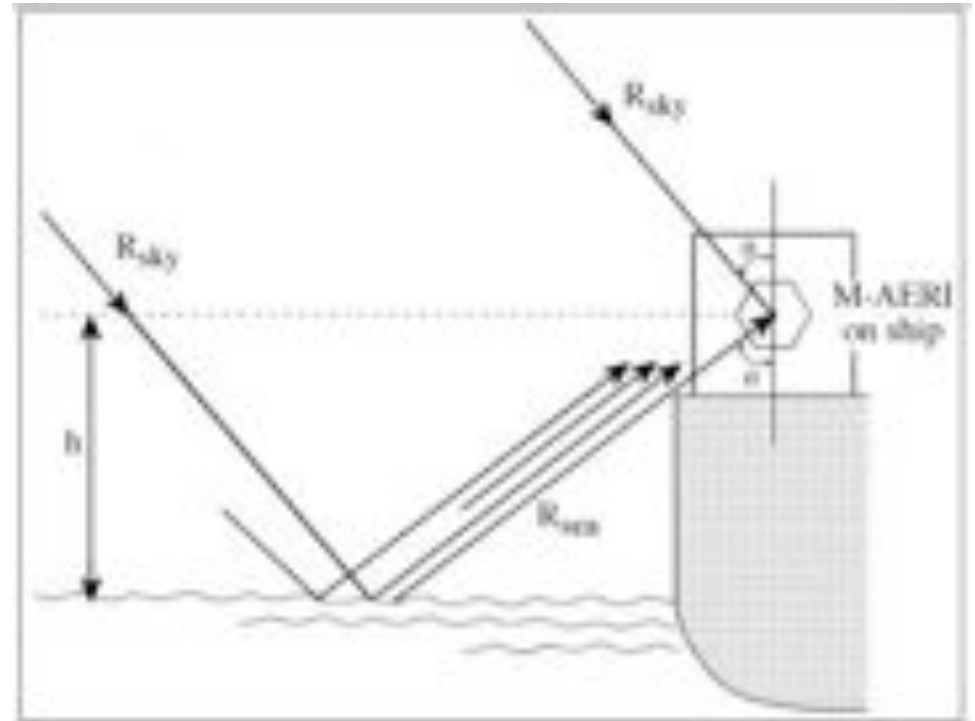


Measuring skin SST from ships

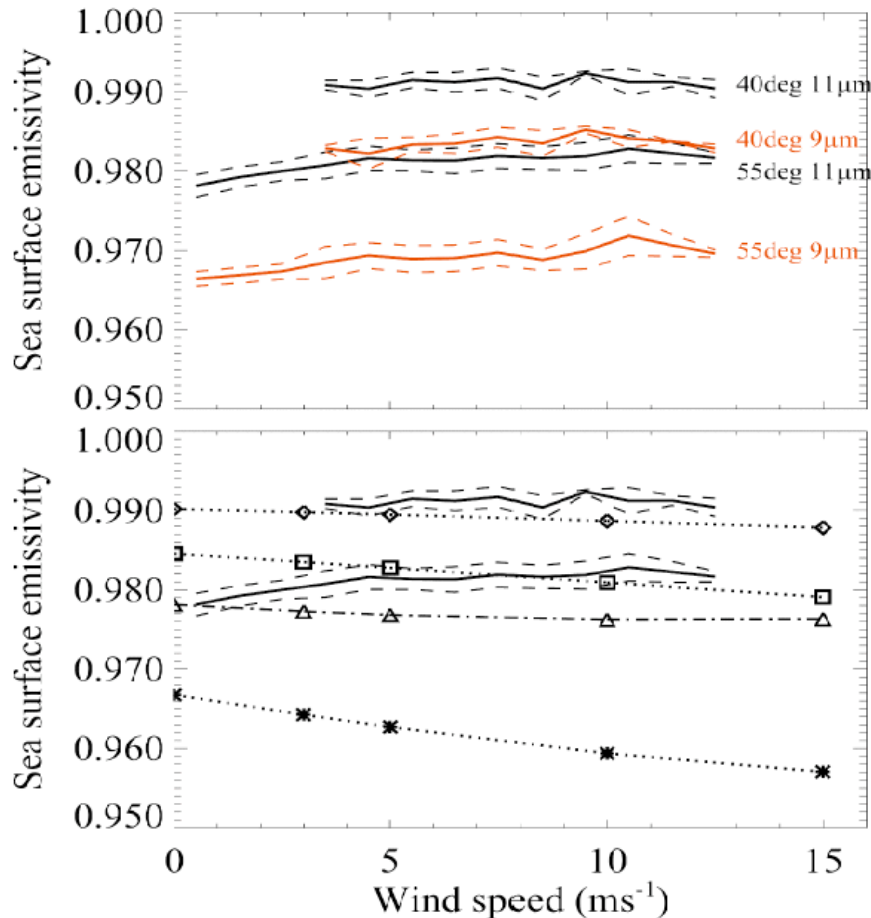
$$R_{\text{water}}(\lambda, \theta) = \varepsilon(\lambda, \theta)B(\lambda, T_{\text{skin}}) \\ + (1 - \varepsilon(\lambda, \theta))R_{\text{sky}}(\lambda, \theta) \\ + R_h(\lambda, \theta)$$

$$T_{\text{skin}} = B^{-1}\langle \{R_{\text{water}}(\lambda, \theta) - [1 - \varepsilon(\lambda, \theta)]R_{\text{sky}}(\lambda, \theta) \\ - R_h(\lambda, \theta)\} / \varepsilon(\lambda, \theta) \rangle$$

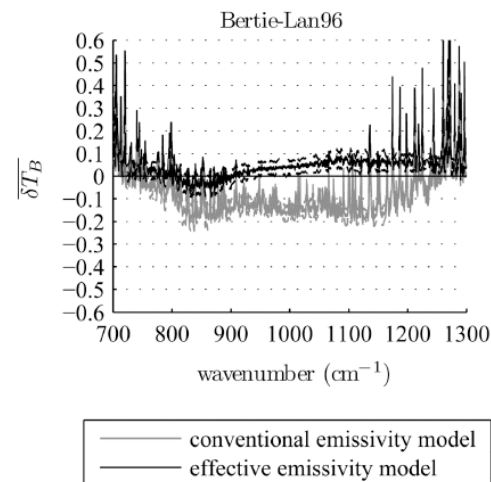
- Scan-mirror mechanism for directing the field of view at complementary angles.
- Excellent calibration for ambient temperature radiances.
- Moderately good calibration at low radiances.



Sea surface emissivity (ϵ)



- Conventional wisdom gave decreasing ϵ with increasing wind.
- Not confirmed by at-sea hyperspectral measurements
- Improved modeling confirms at-sea measurements.

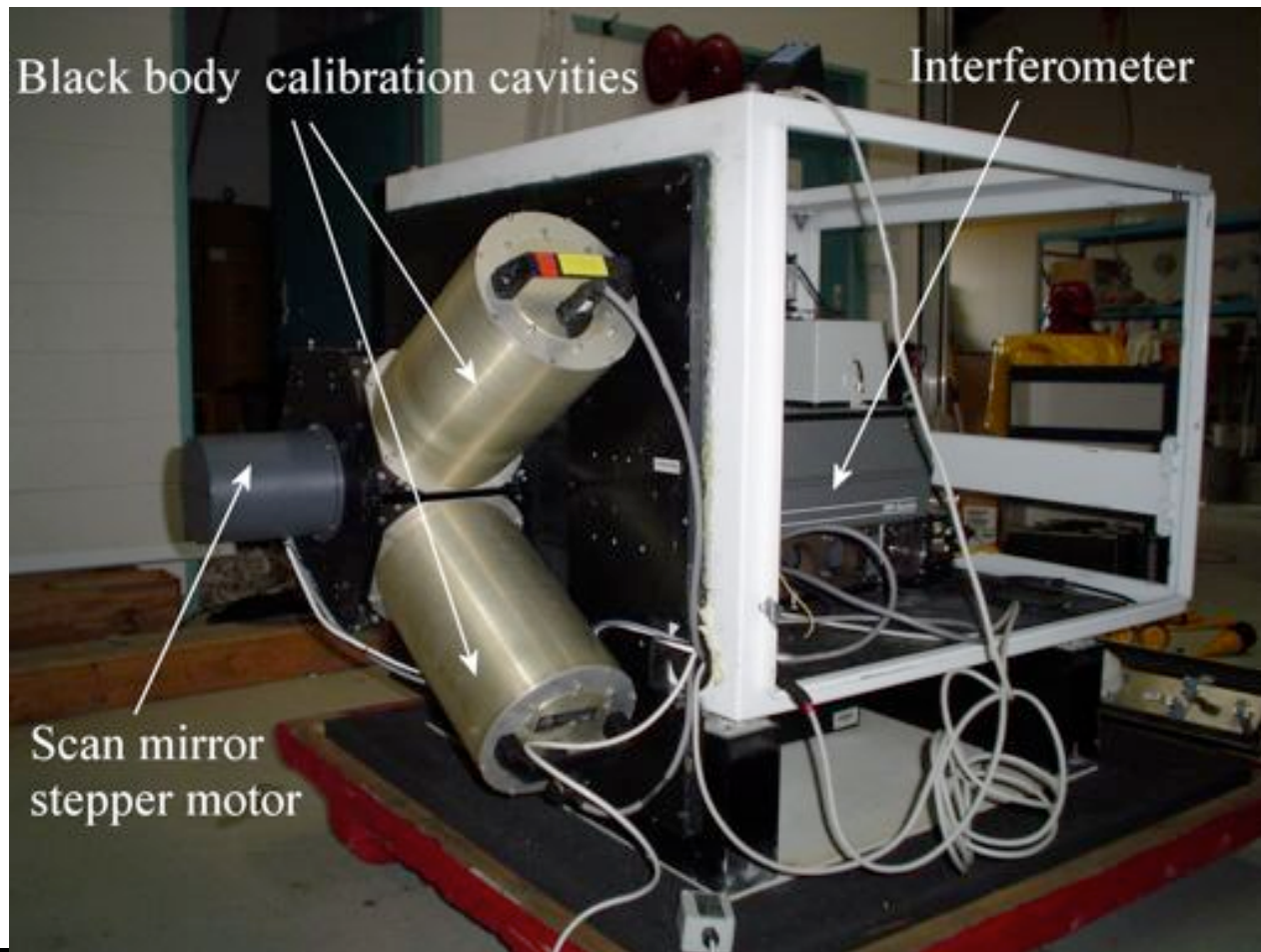


Hanafin, J. A. and P. J. Minnett, 2005: Infrared-emissivity measurements of a wind-roughened sea surface. *Applied Optics*, **44**, 398-411.

Nalli, N. R., P. J. Minnett, and P. van Delst, 2008: Emissivity and reflection model for calculating unpolarized isotropic water surface-leaving radiance in the infrared. I: Theoretical development and calculations. *Applied Optics*, **47**, 3701-3721.

Nalli, N. R., P. J. Minnett, E. Maddy, W. W. McMillan, and M. D. Goldberg, 2008: Emissivity and reflection model for calculating unpolarized isotropic water surface-leaving radiance in the infrared. 2: Validation using Fourier transform spectrometers. *Applied Optics*, **47**, 4649-4671.

Internal Calibration

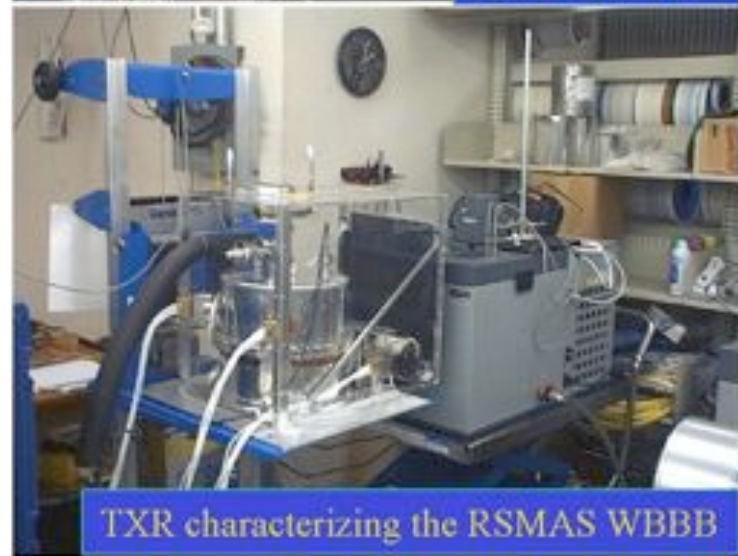


NIST water-bath black-body calibration target



See: Fowler, J. B., 1995. A third generation water bath based blackbody source, *J. Res. Natl. Inst. Stand. Technol.*, 100, 591-599

Traceability to NIST TXR



UNIVERSITY OF MIAMI



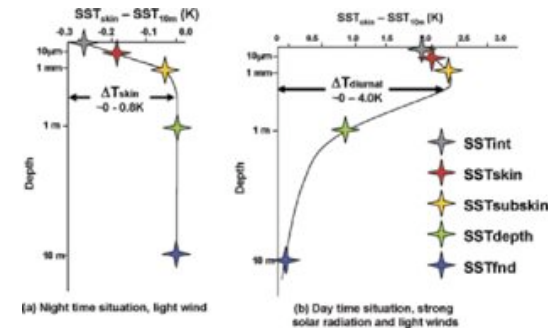
Next-generation ship-based FTIR spectroradiometer



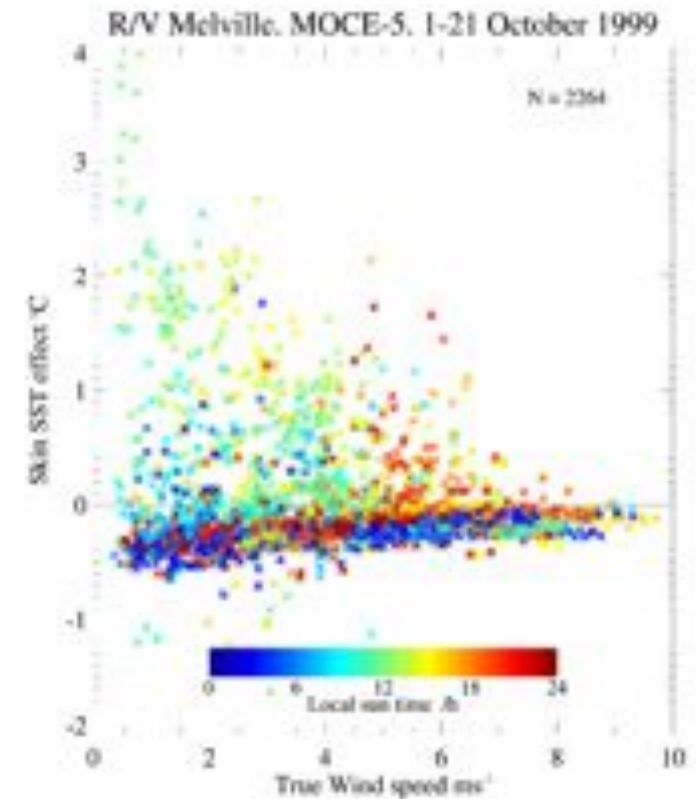
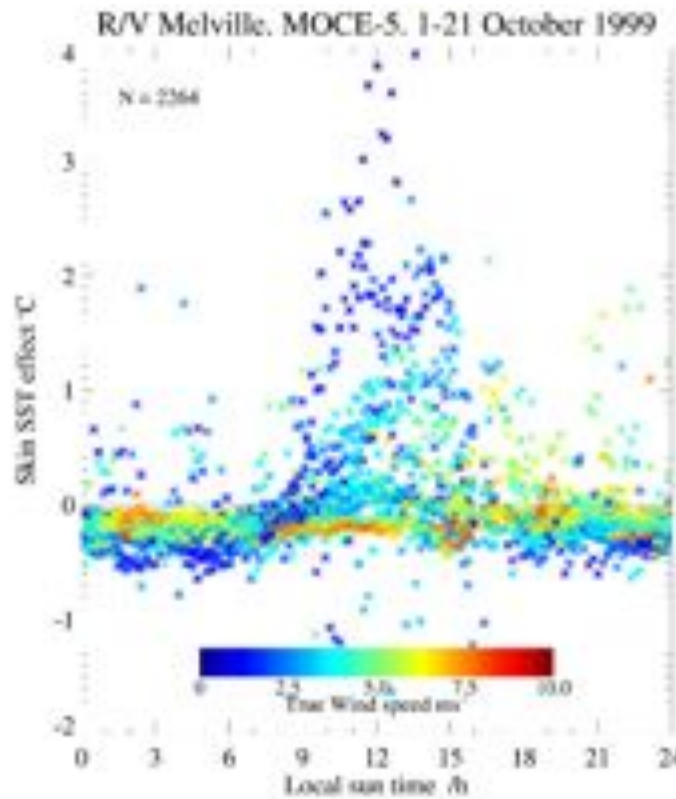
M-AERI Mk-2 undergoing tests at RSMAS.



Skin – bulk SST differences

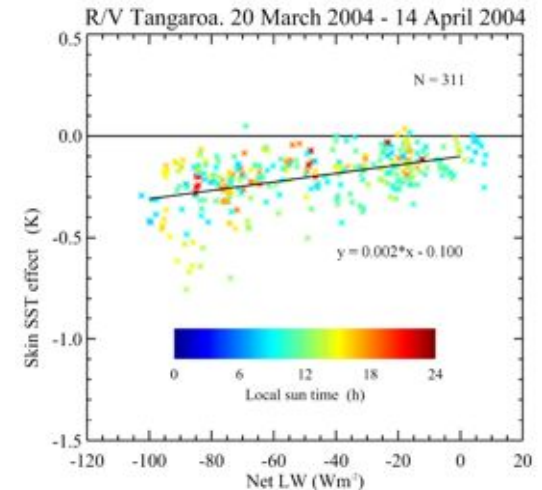
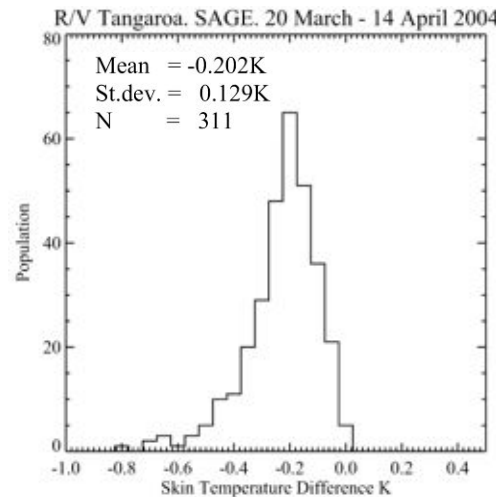
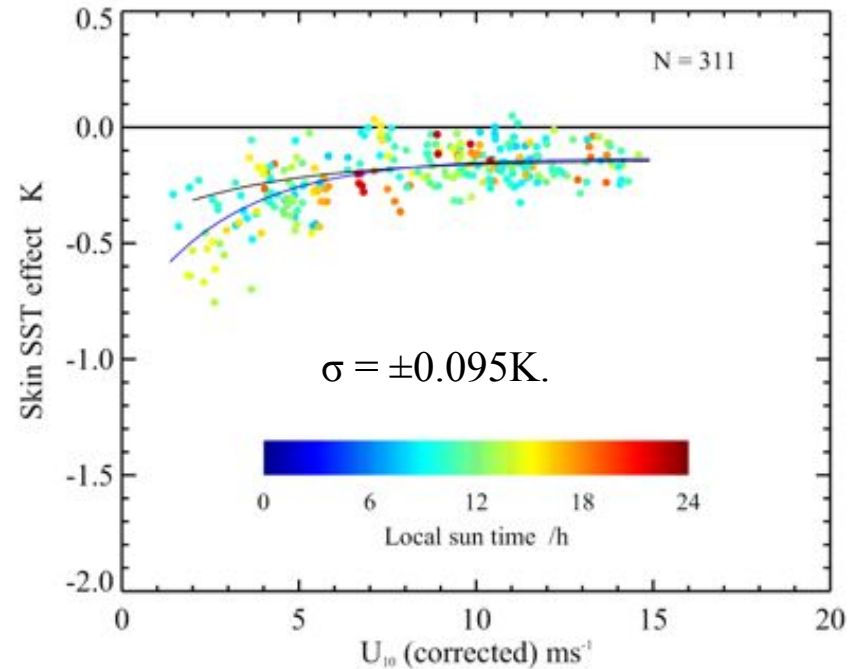


Example of wind speed dependence of diurnal & skin effects – off Baja California



Skin effect

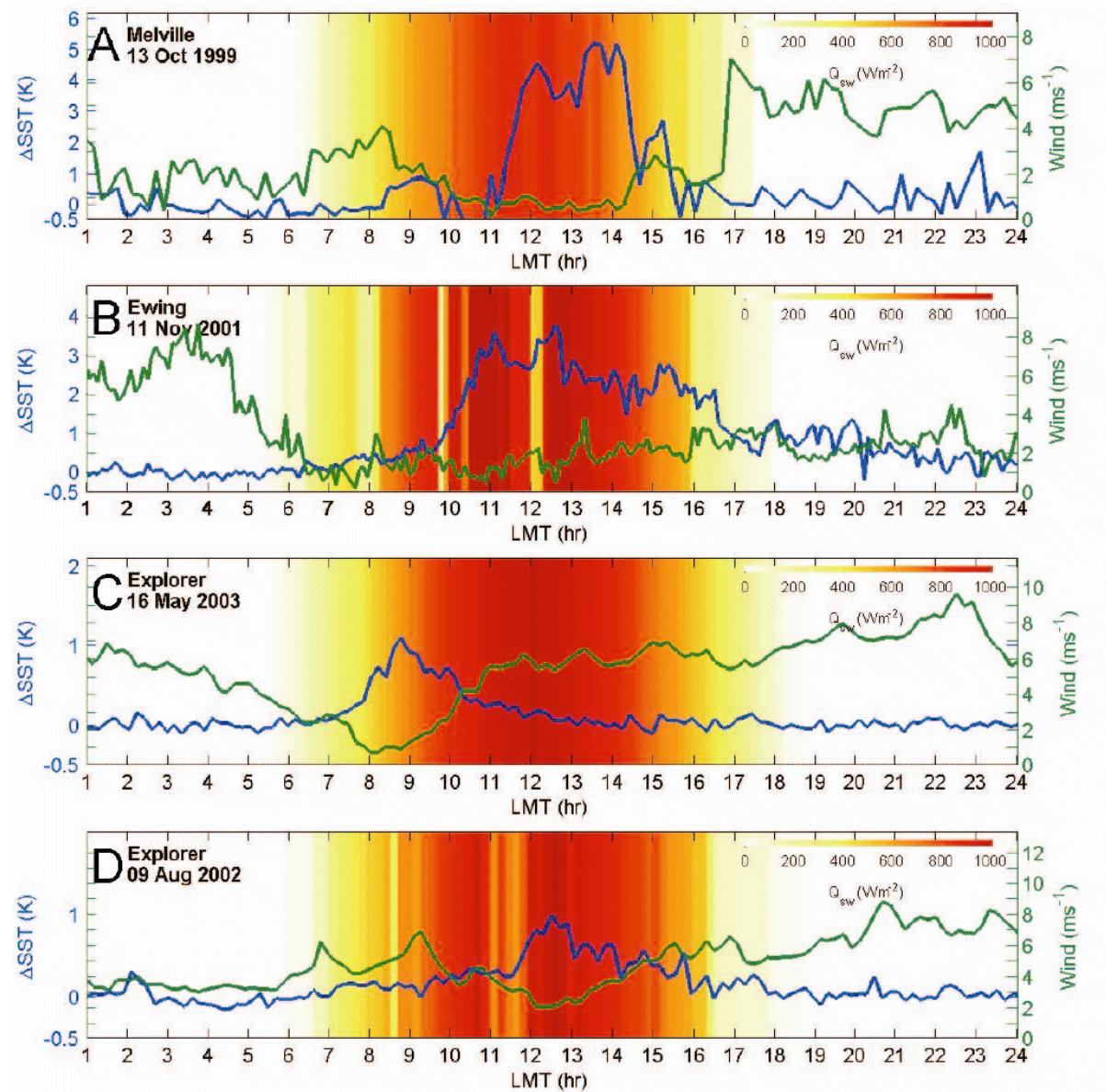
- Caused by molecular conduction being the mechanism for heat flow from ocean to atmosphere.
- First order correction:
 $\Delta T \approx 0.2K$
- Better correction requires:
 - accurate wind-speeds for $U_{10} < 7ms^{-1}$,
 - net infrared heat flux at the surface,
 - incident solar radiation at the surface,
 - SST.



Variability of Diurnal Heating

SST can change significantly in periods of an hour or less.

From Gentemann, C. L. and P. J. Minnett, 2008: Radiometric measurements of ocean surface thermal variability. *Journal of Geophysical Research*, 113, C08017. doi:10.1029/2007JC004540

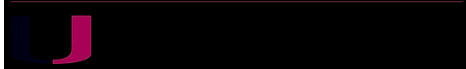
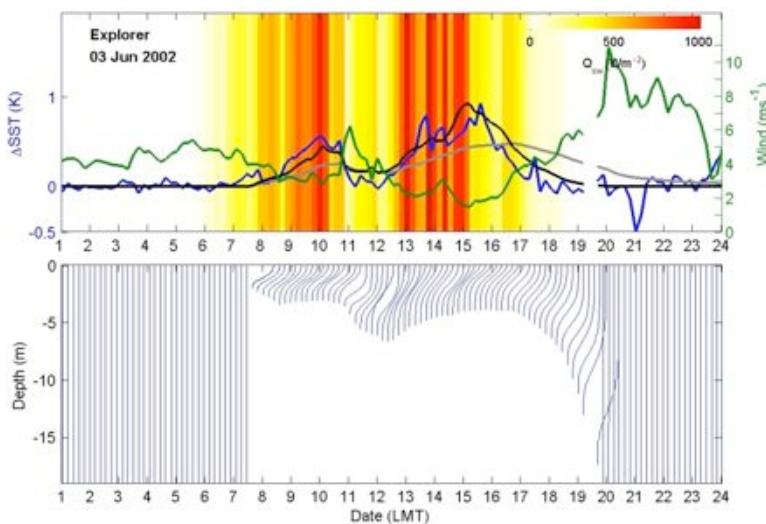
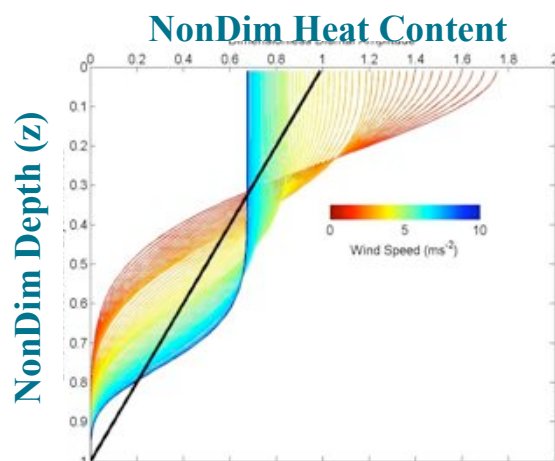


Modeling Diurnal Warming and Cooling

- Prior models generally failed to raise temperatures sufficiently quickly, were not sufficiently responsive to changes in the wind speed, and retained too much heat into the evening and the night.
- New diurnal model that links the advantages of bulk models (speed) with the vertical resolution provided by turbulent closure models.
- Profiles of Surface Heating (POSH) model:

Surface forcing:
(NWP
or in situ)

+



Related activities

- NASA SST Science Team
- NPP (VIIRS) Science Team
- GHRSSST Science Team
- AVHRR Pathfinder Project
- AATSR Science Advisory Group
- HyspIRI Science Study Group
- EUMETSAT Mission Expert Team



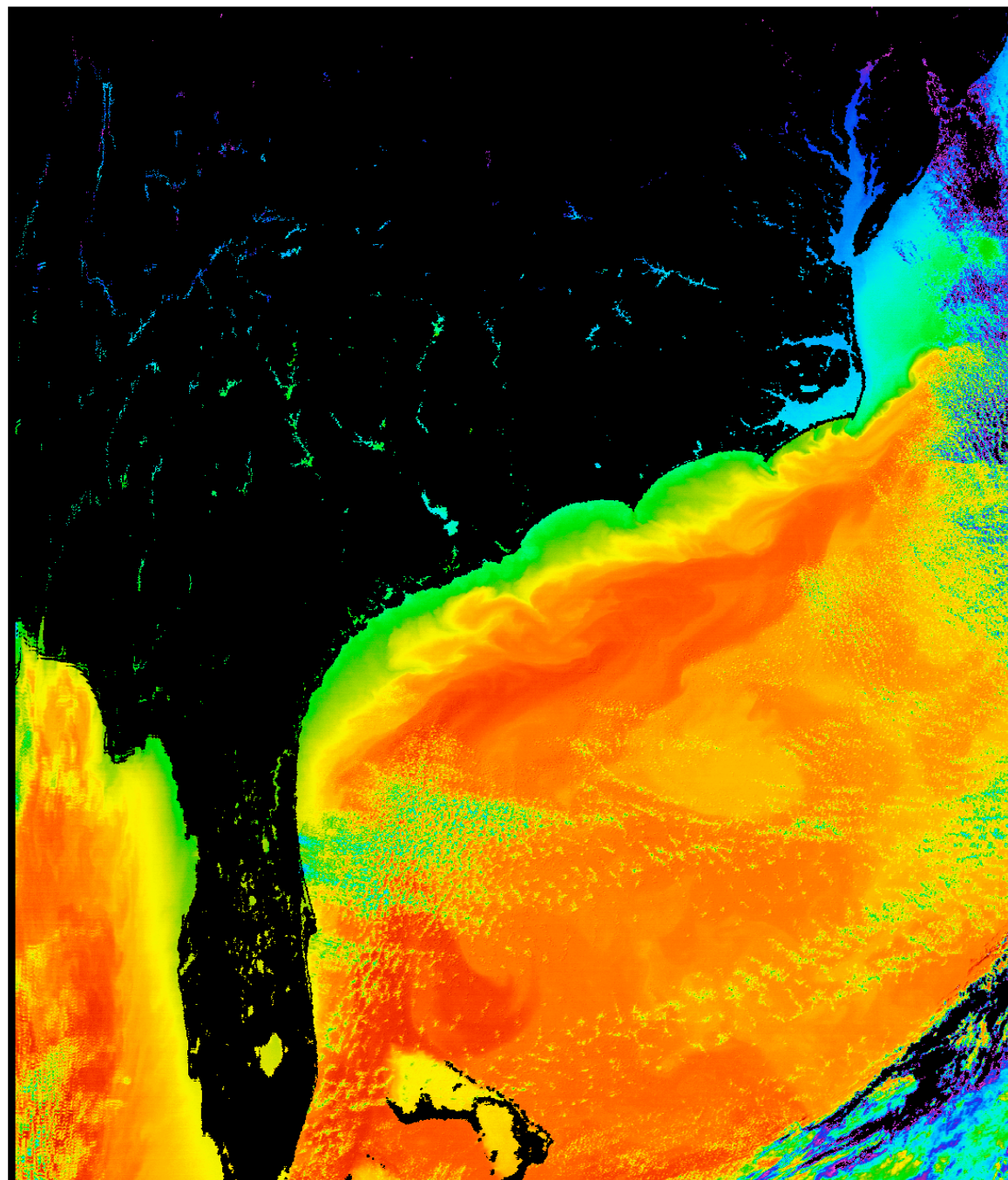
Future

- New ship-based spectroradiometers
 - M-AERI Mk2
- New spacecraft radiometers
 - VIIRS
 - SLSTR
- Better buoy temperatures
 - 0.01K resolution
- Use modified Argo profilers, gliders
 - Measurements up to the surface
- More (autonomous) radiometers, also on UAVs
 - Ball Aerospace have built a miniature a/c radiometer
- Improved atmospheric correction formulations
- “Forward” solution for the atmospheric effect

Thank you for
your attention.

Questions?

Aqua MODIS
SST



0.0 6.0 12.0 18.0 24.0 30.0 ESDIS MYD28L2 sst, Deg C

UNIVERSITY OF MIAMI

